Intermolecular Interactions in *tert*-Butyl Alcohol−Dimethyl Sulfoxide−H_2O: Chemical Potentials, Partial Molar Entropies and Volumes

Christa Trandum,[†,‡] Peter Westh,[†,§,||] Charles A. Haynes,[§] and Yoshikata Koga*[,†]

Department of Chemistry, The University of British Columbia, 2036 Main Mall, Vancouver, B. C. Canada V6T 1Z1, and Biothechnology Laboratory, The University of British Columbia, 6174 University Boulevard, Vancouver, B. C. Canada V6T 1Z3

Received: September 15, 1997; In Final Form: April 9, 1998

The excess chemical potentials, the excess partial molar entropies, and the partial molar volumes in *tert*-butyl alcohol (TBA)−dimethyl sulfoxide (DMSO)−H_2O mixtures were determined. These data, together with previously published excess partial molar enthalpies (*Fluid Phase Equilib.* **1997,** *136,* 207) were used to evaluate intermolecular interactions. The TBA−TBA and TBA−DMSO, and DMSO−DMSO interactions were found to be crucially dependent on the composition. The net interaction in terms of chemical potential is very intricate. For example, net interactions of DMSO with a hydrophobic moiety (represented here by TBA) change from attractive to repulsive as the composition changes. This suggests that general discussions of the affinity of DMSO for nonpolar groups (or surfaces) are meaningful only by specifying the composition region. The interactions in terms of enthalpy and entropy are an order of magnitude larger and strongly compensating. Anomalous changes in the enthalpic/entropic interactions and hence qualitative changes in the mixing scheme of the solution, previously described in respective binary TBA−H_2O and DMSO−H_2O systems, are also apparent in this ternary system. It was found that as the mole fraction, x_D, of DMSO (third component) increases, the transition in mixing scheme occurred at a progressively lower value of x_B . The behavior of partial molar volume indicated that as x_B increases, the initial increase in the partial molar volume of H_2O on increasing x_D, reminiscent to "iceberg formation", diminished. This suggests that existing TBA molecules already made their contribution to the "iceberg formation". The DMSO−DMSO interaction in terms of volume also showed that the transition occurred at a smaller value of x_D than that for $x_B = 0$. The boundary between the two mixing schemes in the present ternary mixture was a straight line in the x_D−x_B field, suggesting that the effect of TBA and DMSO on H_2O, causing the transition in the mixing scheme, is additive.

Introduction

Thermodynamic quantities proportional to higher order derivatives of Gibbs energy, *G*, contain increasingly detailed physical information. Use of such quantities therefore provide a powerful, but largely ignored, model-free approach to elucidate mixing schemes or local "structure" in liquid mixtures.[1−8] This is particularly true for systems containing H_2O that are known to have a complex molecular organization very sensitive to the addition of solutes.[1−9] Previously, we have reported excess partial molar quantities (second derivatives of *G*) for binary aqueous solutions of *tert*-butyl alcohol (abbreviated as TBA, hereinafter),[1−5] and dimethyl sulfoxide (DMSO).[6] They were measured directly, accurately and in small increments in the mole fraction of solute. Therefore we were able to evaluate the derivative once more with respect to the mole fraction, i.e., third derivatives of *G*. We suggested that these composition derivatives of the excess partial molar quantities signify the strength of the solute−solute interactions. Combining these data with those of similar studies on other aqueous nonelectrolytes, we proposed that there are three composition regions, in each of which the mixing schemes are qualitatively different from those of other regions.[1−8] In the most water-rich region, all the above data are consistent with a molecular arrangement, called "mixing scheme I", in which well-separated solute molecules enhance the hydrogen bond network of solvent water in their immediate vicinities but reduce the hydrogen bond probability in the bulk away from the solutes. Even so, the bond-percolation nature[9,10] of the hydrogen bond network is retained. Via this percolated hydrogen bond network, well-separated solutes interact with each other repulsively in terms of enthalpy, but attractively entropywise. When the concentration of solute increases, the hydrogen bond probability of the bulk water progressively decreases until the percolation threshold is reached. At this point, the solvent water loses its bond-percolation nature, and a new mixing scheme, II, sets in. Mixing scheme II may typically be understood as consisting of two kinds of clusters rich in each component. The solute−solute interactions were found an order of magnitude weaker than those in mixing scheme I and operative locally within each clusters.[1−8] Finally, in the solute-rich region, bulk water structure is completely lost, forcing individual water molecules to interact with the clusters of solute molecules (mixing scheme III). The boundary between mixing schemes I and II is associated with

* Correspondence should be addressed to this author.
† Department of Chemistry, The University of British Columbia.
‡ Present address: Department of Physical Chemistry, Technical University of Denmark, DK-2800 Lyngby, Denmark.
§ Biotechnology Laboratory, The University of British Columbia.
|| Present address: Department of Chemistry, Roskilde University, DK-4000, Roskilde, Denmark.

S1089-5647(97)03021-6 CCC: $15.00
Published on Web 06/05/1998

TABLE 1: Measured Vapor Pressures

x_D	x_B	t/°C	p/Torr	x_D	x_B	t/°C	p/Torr
			$x_D^0 = 0.0$				
0.0	0.0000	24.951	23.708	0.0	0.0083	24.950	27.572
0.0	0.0177	24.951	31.493	0.0	0.0268	24.952	35.179
0.0	0.0364	24.952	38.756	0.0	0.0446	24.953	41.257
0.0	0.0540	24.953	43.260	0.0	0.0631	24.952	44.417
0.0	0.0721	24.952	45.088	0.0	0.0859	24.949	45.641
0.0	0.1002	24.952	45.998				
			$x_D^0 = 0.340$				
0.0340	0.0000	24.949	22.975	0.0337	0.0072	24.949	26.340
0.0334	0.0165	24.949	30.416	0.0332	0.0248	24.949	33.946
0.0329	0.0338	24.949	37.442	0.0325	0.0438	24.951	40.536
0.0322	0.0525	24.950	42.352	0.0319	0.0616	24.950	43.517
0.0316	0.0719	24.950	44.321	0.0312	0.0832	24.950	44.833
0.0307	0.0982	24.952	45.280	0.0301	0.1172	24.949	45.596
			$x_D^0 = 0.1033$				
0.1033	0.0000	24.948	20.823	0.1028	0.0059	24.950	23.810
0.1021	0.0123	24.946	26.858	0.1015	0.0189	24.946	29.939
0.1008	0.0258	24.945	32.860	0.1000	0.0334	24.945	35.692
0.0992	0.0416	24.945	38.028	0.0984	0.0501	24.945	39.656
0.0973	0.0607	24.944	41.077	0.0961	0.0729	24.945	42.068
0.0946	0.0875	24.945	42.766	0.0932	0.1015	24.946	43.131
0.0918	0.1152	24.946	43.460				
			$x_D^0 = 0.1577$				
0.1577	0.0000	24.947	18.609	0.1568	0.0061	24.946	21.742
0.1558	0.0124	24.948	24.944	0.1546	0.0201	24.946	28.322
0.1534	0.0279	24.946	31.350	0.1523	0.0352	24.949	33.620
0.1511	0.0431	24.948	35.563	0.1496	0.0522	24.947	37.201
0.1481	0.0618	24.946	38.429	0.1466	0.0717	24.946	39.235
0.1449	0.0824	24.947	39.916	0.1432	0.0934	24.947	40.473
0.1443	0.1055	24.948	40.885	0.1389	0.1207	24.947	41.338
			$x_D^0 = 0.2344$				
0.2344	0.0000	24.950	14.970	0.2342	0.0010	24.949	15.478
0.2331	0.0063	24.947	18.060	0.2318	0.0122	24.947	20.772
0.2304	0.0187	24.946	23.409	0.2288	0.0259	24.948	25.954
0.2269	0.0343	24.950	28.328	0.2250	0.0429	24.948	30.258
0.2226	0.0532	24.948	31.942	0.2202	0.0639	24.948	33.253
0.2169	0.0784	24.950	34.569	0.2135	0.0931	24.950	35.454
0.2105	0.1062	24.950	36.075	0.2076	0.1189	24.949	36.539
			$x_D0 = 0.3182$				
0.3182	0.0000	24.950	11.449	0.3169	0.0047	24.951	13.470
0.3155	0.0095	24.951	15.275	0.3134	0.0166	24.952	17.761
0.3112	0.0238	24.952	19.908	0.3084	0.0332	24.950	22.296
0.3054	0.0430	24.952	24.279	0.3019	0.0545	24.949	26.091
0.2980	0.0673	24.951	27.612	0.2938	0.0806	24.953	28.833
0.2896	0.0945	24.953	29.839	0.2851	0.1091	24.952	30.636
0.2808	0.1232	24.954	31.304				
			$x_D0 = 0.3877$				
0.3877	0.0000	24.950	9.033	0.3853	0.0068	24.950	11.303
0.3820	0.0159	24.950	14.008	0.3789	0.0243	24.950	16.039
0.3758	0.0329	24.950	17.847	0.3728	0.0411	24.949	19.295
0.3696	0.0498	24.950	20.646	0.3661	0.0595	24.949	21.894
0.3622	0.0700	24.950	22.874	0.3588	0.0792	24.950	23.758
0.3548	0.0900	24.948	24.612	0.3511	0.1001	24.949	25.340
0.3473	0.1105	24.947	25.970	0.3439	0.1201	24.948	26.486

anomalies in the third derivatives of G,[1−8] while fourth derivative anomalies are indicative of the transition between II and III.[4,6]

Previous studies indicate that for TBA−H_2O, the entropic attraction among TBA molecules is stronger than enthalpic repulsion, resulting in net attraction in terms of chemical potential.[1−5,7,8] For DMSO−H_2O, on the other hand, the enthalpic repulsion surpasses the entropic attraction leading to net repulsion among DMSO molecules in terms of chemical potential.[6−8] In both cases, the strength of the solute−solute interaction in terms of chemical potential is smaller by an order of magnitude than the enthalpic and the entropic contribution. This is a manifestation of the enthalpy−entropy compensation effect, which has been generally observed in aqueous solutions of nonelectrolytes.[11] Hence, subtleties in the behavior of chemical potential may become much more conspicuous when the constituent partial molar enthalpy and partial molar entropy are separately determined.

Among other thermodynamic data proportional to the second derivatives of G, the partial molar volume data were also proved to be useful in support of the above interpretations.[6−8,12] In particular, the partial molar volume of solute in TBA−H_2O,[12] DMSO−H_2O,[6] and 2-butoxyethanol (BE)−H_2O[13,14] shows an initial decrease on increasing the solute concentration in mixing scheme I. This is equivalent, due to the Gibbs−Duhem relation, to an initial increase in the partial molar volume of H_2O, indicating the formation of icelike patches due to introduction of a hydrophobic solute. The composition derivatives of the partial molar volume (a third derivative of G), i.e. the influence of an incoming solute on the partial molar volume of the existing solute, showed anomalies at the same boundary from mixing scheme I to II.[6,12−14]

In this paper, we present the following data for a ternary system, TBA−DMSO−H_2O; the excess chemical potential, μ_i^E, (i = TBA or DMSO), the excess partial molar entropies, S_i^E, calculated using the excess partial molar enthalpies, H_i^E,[16] and the partial molar volumes, V_i^E. We then evaluate the composition derivatives of these partial molar quantities and discuss intermolecular interactions among solute molecules and their influences in the hydrogen bond network of solvent water. Earlier, we discussed the solute−solute interactions in this ternary system using the H_i^E data alone.[16] In this work, we supplement such discussions by using μ_i^E, S_i^E, and V_i^E data and thus make an attempt to deepen the understandings on the intermolecular interactions in DMSO−TBA−H_2O.

Experimental Section

The total pressures of the mixture were determined by a static method described elsewhere.[4,5,15,25] *tert*-Butyl alcohol (Aldrich, 99.5 + %) and dimethyl sulfoxide (Aldrich, 99.9%) were used as supplied. H_2O was triply distilled; last distilled in glass immediately before use. The total vapor pressure data are given in Table 1. The numerical method of calculating the partial pressures from them is shown in Appendix I. The resulting partial pressures are listed in Table 3.

For density measurements, *tert*-butyl alcohol (99%) was obtained from Sigma, and dimethyl sulfoxide (99.5%) was obtained from Merck. H_2O was doubly distilled in a quartz still immediately before use. An automatic vibrating-tube densimeter was described elsewhere.[13] Various series of binary mixtures TBA−H_2O were prepared. Then automatically a small amount of DMSO was successively added and the density was determined.

Table 5 shows the measured density, d, as a function of mole fractions, x_D, and x_B. The partial molar volume of DMSO, V_D, was calculated as

$$V_D = \delta V/\delta n_D \tag{1}$$

$$\delta V = \{(\sum M_k n_k)/d\}_{aft} - \{(\sum M_k n_k)/d\}_{bef} \tag{2}$$

where M_k is the molecular weight of the kth component, n_k its molar amount, and d the density and the subscripts "bef" and "aft" signify before and after a small amount of DMSO, δn_D, is added. Except for some sporadic scatters, which perhaps due to particular contamination off the rubber tubing in the densimeter system, the uncertainty on V_D was ±0.15 cm^3 mol^{-1}.

TABLE 2: Vapor Pressures, *p*/Torr, at Fixed Values of x_D and x_B at 24 95 °C (±0.01 Torr)

	x_B																			
x_D	0.0	0.005	0.01	0.015	0.02	0.025	0.03	0.035	0.04	0.045	0.05	0.055	0.06	0.07	0.08	0.09	0.1	0.11	0.12
0.0	23.68	26.07	28.28	30.37	32.34	34.43	36.43	38.27	39.91	41.32	42.49	43.39	44.07	44.93	45.44	45.79	45.96	46.07	46.14
0.01	23.52	25.88	28.11	30.25	32.27	34.38	36.38	38.22	39.86	41.25	42.39	43.26	43.92	44.77	45.28	45.64	45.80	45.92	45.98
0.03	23.11	25.45	27.74	29.96	32.05	34.19	36.18	38.02	39.62	40.97	42.04	42.88	43.49	44.33	44.84	45.23	45.37	45.51	45.56
0.05	22.60	24.95	27.29	29.59	31.73	33.87	35.84	37.66	39.22	40.52	41.53	42.33	42.92	43.75	44.26	44.66	44.81	44.97	45.03
0.07	21.99	24.37	26.78	29.13	31.30	33.43	35.37	37.15	38.66	39.89	40.86	41.63	42.19	43.02	43.54	43.95	44.12	44.30	44.37
0.09	21.31	23.73	26.19	28.57	30.76	32.87	34.76	36.49	37.94	39.11	40.03	40.78	41.32	42.15	42.69	43.10	43.30	43.49	43.59
0.11	20.55	23.02	25.51	27.91	30.11	32.17	34.01	35.69	37.08	38.09	39.07	39.79	40.33	41.16	41.71	42.12	42.36	42.56	42.69
0.13	19.75	22.25	24.76	27.16	29.34	31.35	33.13	34.76	36.07	37.12	37.98	38.68	39.21	40.04	40.61	41.03	41.30	41.50	41.66
0.15	18.89	21.42	23.93	26.31	28.46	30.40	32.14	33.69	34.94	35.94	36.77	37.45	37.98	38.82	39.41	39.83	40.13	40.34	40.52
0.17	18.01	20.54	23.03	25.37	27.48	29.35	31.03	32.51	33.70	34.65	35.46	36.13	36.66	37.51	38.11	38.53	38.86	39.08	39.28
0.19	17.10	19.61	22.07	24.35	26.40	28.20	29.82	31.22	32.35	33.28	34.07	34.72	35.25	36.11	36.72	37.16	37.50	37.73	37.94
0.21	16.18	18.66	21.05	23.26	25.24	26.96	28.53	29.86	30.93	31.83	32.60	33.24	33.78	34.64	35.27	35.72	36.06	36.31	36.53
0.23	15.25	17.67	19.99	22.11	24.01	25.66	27.16	28.42	29.44	30.32	31.08	31.71	32.25	33.11	33.75	34.22	34.57	34.83	35.05
0.25	14.34	16.68	18.90	20.93	22.74	24.31	25.75	26.94	27.91	28.78	29.52	30.15	30.69	31.55	32.20	32.68	33.03	33.31	33.53
0.27	13.44	15.69	17.79	19.72	21.44	22.93	24.31	25.43	26.37	27.22	27.95	28.57	29.11	29.97	30.62	31.12	31.47	31.76	31.98
0.29	12.57	14.71	16.70	18.52	20.14	21.56	22.87	23.93	24.83	25.67	26.39	27.00	27.53	28.39	29.04	29.55	29.91	30.21	30.44
0.31	11.74	13.77	15.62	17.34	18.86	20.21	21.45	22.46	23.33	24.15	24.85	25.46	25.98	26.83	27.48	28.00	28.37	28.68	28.91
0.33	10.96	12.87	14.60	16.21	17.64	18.92	20.08	21.04	21.89	22.68	23.36	23.96	24.46	25.31	25.95	26.47	26.87	27.18	27.44
0.35	10.23	12.04	13.66	15.17	16.51	17.72	18.80	19.72	20.54	21.29	21.95	22.54	23.02	23.86	24.49	24.98	25.44	25.75	26.05

For the series for the initial mole fraction of TBA, $x_B^0 = 0.01870$, the uncertainty was less than ± 0.1 $cm^3 mol^{-1}$.

Results

To obtain partial pressures from the total vapor pressure data, we adopted a numerical method based on the Gibbs−Duhem relation. On account of the singular behavior at the boundary of mixing scheme indicated by the partial molar enthalpy data,[16] we did not choose to use the usual method of utilizing an everywhere analytical fitting function for G^E.[29] The detail is shown in Appendix I. The excess chemical potential of the i-th component, μ_i^E, is calculated using the partial pressure data, p_i, at 24.95 °C, given in Table 3 by

$$\mu_i^E = RT \ln\{p_i/(x_i p_i^0)\} \quad (3)$$

where p_i^0 is the vapor pressure of pure i (= B or D) at the same temperature. Note that the gas-phase nonideality is negligible in comparison with the liquid-phase nonideality. μ_B^E and μ_D^E are plotted in Figure 1. As mentioned in Appendix I, the uncertainties in μ_B^E and μ_D^E are estimated to be ±0.03 kJ mol^{-1} at the worst but more likely better by at least 10-fold. From the data of μ_i^E at 24.95 °C and those of H_i^E at 26.90 °C reported earlier,[16] the values of S_i^E at 26.90 °C were calculated. First, however, the data of μ_i^E were converted to those at 26.90 °C by the correction, $\delta(\mu_i^E/T) = -(H_i^E/T^2)\delta T$. The uncertainty in TS_B^E is estimated to be ±0.05 kJ mol^{-1} and that for TS_D^E is ± 0.3 kJ mol^{-1}, similar to that in H_i^E.[16] Figure 2 shows the plots of TS_i^E (filled symbols) together with smoothed values of H_i^E [16] (hollow symbols). By comparison of Figures 1a,b and 2a or Figures 1c and 2b, it is evident that the enthalpy−entropy compensation is operative as generally observed in aqueous solutions.[11]

The detailed picture we drew in the Introduction on mixing schemes in the respective binary aqueous solutions originated from such data as shown in Figures 1 and 2. The line of logic we use is detailed in the previous papers,[1−8] which is repeated below briefly.

For TBA, in all cases shown in Figure 2a the values of TS_B^E are more negative than H_B^E at a given value of x_D^0, the initial composition of DMSO. As a result, the values of μ_B^E remain positive in the range studied (parts a and b of Figure 1). When dilute, incoming TBA molecules settle in the solution with a large enthalpy gain and a larger entropy loss (Figure 2a). This can be attributed to the so-called "iceberg formation" in the vicinity of the solute.[1−5,7,8] As the concentration of TBA increases, the degree of enthalpy gain and entropy loss becomes smaller. Namely, the enthalpic situation becomes less favorable, while the entropic situation becomes less unfavorable. This concept lead us earlier to introduce "interaction functions" basically as a slope of the partial molar quantities,[1−8] as will be discussed below. Thus, the effect of incoming solute is felt in the mixture by a lesser degree because the hydrogen bond network has already been modified. As x_D^0 increases, these effects on the thermodynamic situation of TBA become progressively smaller, hinting that both DMSO and TBA modify the hydrogen bond network of H_2O in a similar manner.

We note in Figure 2a that for $x_D^0 = 0$ (a binary TBA−H_2O), the slopes of H_B^E and TS_B^E become progressively larger as x_B increases from 0 to about 0.05; thereupon, the slope becomes almost zero rather suddenly above 0.07. This lead us earlier to realize a qualitative change in mixing schemes, from I to II, as mentioned in Introduction. As is evident in Figure 2a, such a transition becomes less drastic and occurs at a smaller value of x_B, as x_D^0 increases. This point will be discussed in more detail below.

The behavior of μ_B^E, Figure 1a, is the result of the competition between the above enthalpy/entropy effects. Figure 1a indicates that generally μ_B^E becomes less positive as x_B increases, indicating a more favorable situation in terms of the chemical potential at a higher composition of TBA molecules. The dependence of μ_B^E on x_D appears more intricate, as shown in Figure 1b. The effect of DMSO on μ_B^E and that of TBA on μ_D^E are generally small as seen in parts b and c of Figure 1. However, their effects are actually drastic as evidenced by the behaviors of the constituent H_i^E and TS_i^E data (Figure 2). This is another manifestation of entropy/enthalpy compensation. We point out that the chemical potential is a first derivative of G, while partial molar enthalpy and entropy are second-order derivatives.

The situation for DMSO is similar except that a large enthalpy gain surpasses the entropy loss. (Figure 2b) As a result, μ_D^E is negative (Figure 1c). This difference from TBA could be attributed to the difference in the relative strength in hydrophobic vs hydrophilic moieties of each solute. However, a more

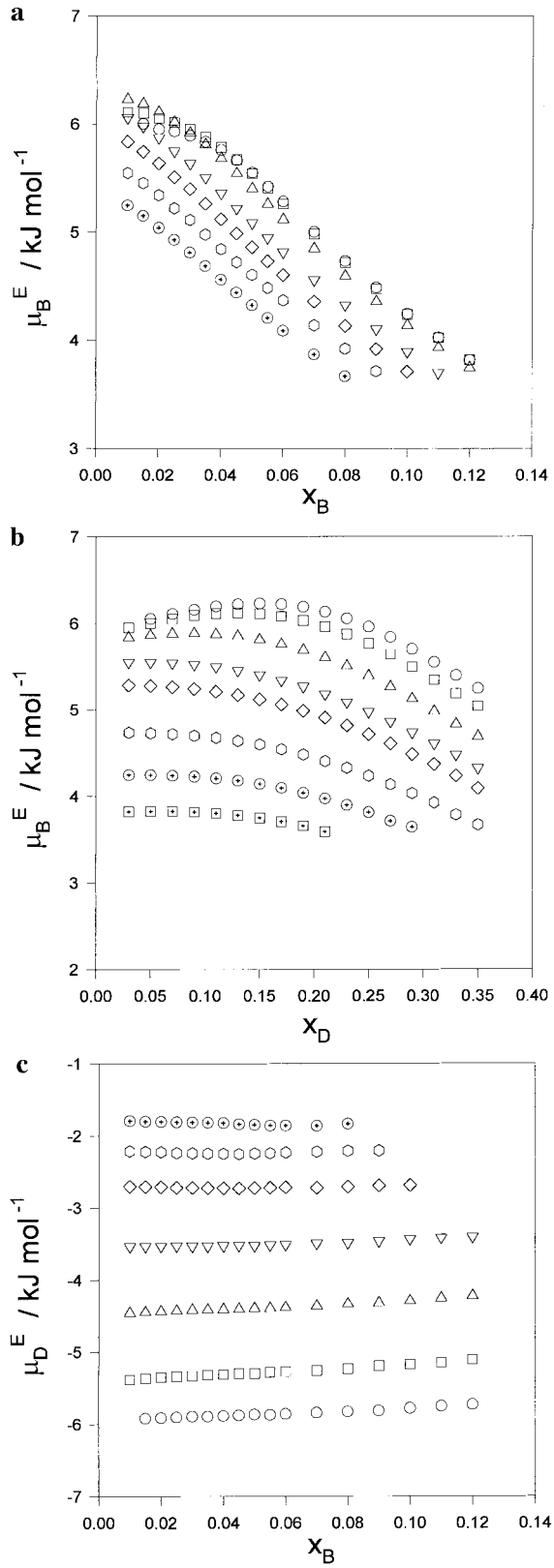

Figure 1. (a) Excess chemical potential of TBA, μ_B^E at 24.95 °C, as a function of the mole fraction of TBA, x_B, for selected values of the mole fraction of DMSO, x_D: (○) 0.03; (□) 0.07; (△) 0.15; (▽) 0.23; (◇) 0.27; (⬡) 0.31; (plus in circle) 0.35. (b) Excess chemical poteitial of TBA, μ_B^E at 24.95 °C, as a function of the mole fraction of DMSO, x_D, for selected values of the mole fraction of TBA, x_B: (○) 0.01; (□) 0.02; (△) 0.035; (▽) 0.05; 0.06; (⬡) 0.08; (plus in circle) 0.1; (plus in square) 0.12. (c) Excess chemical potential of DMSO, μ_D^E, at 24.95 °C as a function of x_B, for selected values of x_D: (○) 0.03; (□) 0.09; (△) 0.15; (▽) 0.21, (◇) 0.27; (⬡) 0.31; (plus in circle) 0.35.

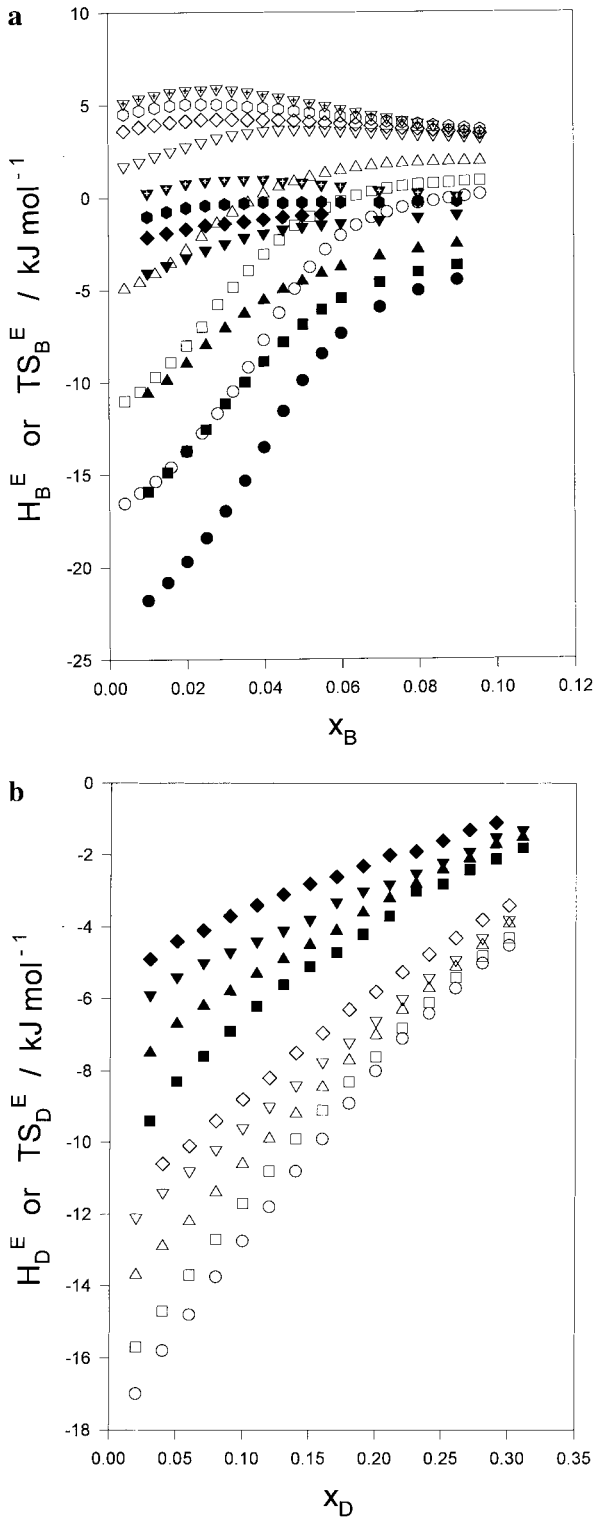

Figure 2. (a) Excess partial molar enthalpy, H_B^E (hollow symbols), and entropy, S_B^E (filled symbols), of TBA for selected values of x_D^0: (○) 0; (□) 0.0478; (△) 0.1031; (▽) 0.1999; (◇) 0.2341; (⬡) 0.2735; (plus in triangle) 0.3540. (b) Excess partial molar enthalpy, H_D^E (hollow symbols), and entropy, S_D^E (filled symbols), of DMSO for selected values of x_B^0: (○) 0; (□) 0.00954; (△) 0.0302; (▽) 0.0507; (◇) 0.0724.

detailed discussion must wait for further study including that by X-ray scattering.[28]

Discussions

Chemical Potentials. We argued earlier[1−8] that the derivative of μ_i^E with respect to n_j, eq 4 below, is an indication of the

TABLE 3: Partial Pressures, p_i/Torr (i = B, D, or W)

		x_B																			
x_D		0.0	0.005	0.01	0.015	0.02	0.025	0.03	0.035	0.04	0.045	0.05	0.055	0.06	0.07	0.08	0.09	0.10	0.11	0.12
0.0	p_W	*23.68*	*23.62*	*23.50*	*23.39*	*23.28*	*23.16*	*23.05*	*22.95*	*22.85*	*22.77*	*22.69*	*22.63*	*22.59*	*22.52*	*22.47*	*22.44*	*22.42*	*22.41*	*22.40*
	p_D	*0.0*	*0.0*	*0.0*	*0.0*	*0.0*	*0.0*	*0.0*	*0.0*	*0.0*	*0.0*	*0.0*	*0.0*	*0.0*	*0.0*	*0.0*	*0.0*	*0.0*	*0.0*	*0.0*
	p_B	*0.0*	*2.448*	*4.775*	*6.981*	*9.060*	*11.27*	13.38	*15.32*	*17.06*	*18.56*	*19.80*	*20.75*	*21.48*	*22.41*	*22.97*	*23.35*	*23.54*	*23.66*	*23.74*
0.01	p_W	*23.52*	*23.46*	*23.34*	*23.22*	*23.11*	*22.99*	*22.88*	*22.78*	*22.68*	*22.60*	*22.53*	*22.47*	*22.42*	*22.36*	*22.31*	*22.28*	*22.26*	*22.25*	*22.24*
	p_D	*0.000649*	*0.000649*	*0.000666*	*0.000669*	*0.000672*	*0.000674*	*0.000676*	*0.000679*	*0.000681*	*0.000683*	*0.000683*	*0.000686*	*0.000687*	*0.000690*	*0.000693*	*0.000698*	*0.000700*	*0.000703*	*0.000709*
	p_B	*0.0*	*2.421*	*4.774*	*7.030*	*9.154*	*11.39*	*13.50*	*15.44*	*17.17*	*18.65*	*19.86*	*20.79*	*21.49*	*22.41*	*22.97*	*23.36*	*23.54*	*23.67*	*23.74*
0.03	p_W	*23.11*	*23.05*	*22.90*	22.78	22.67	22.55	22.43	22.33	22.24	22.15	22.08	22.03	21.98	21.91	21.86	21.82	21.79	21.77	21.75
	p_D	*0.001608*	*0.001608*	*0.001667*	0.001665	0.001670	0.001675	0.001683	0.001684	0.001689	0.001694	0.001701	0.001700	0.001708	0.001719	0.001731	0.001738	0.001763	0.001784	0.001799
	p_B	*0.0*	*2.400*	*4.839*	7.181	9.380	11.64	13.74	15.68	17.38	18.82	19.95	20.84	21.58	22.42	22.98	23.40	23.57	23.75	23.81
0.05	p_W	*22.59*	*22.53*	22.41	22.28	22.16	22.03	21.92	21.81	21.72	21.63	21.57	21.51	21.47	21.39	21.34	21.28	21.25	21.21	21.18
	p_D	*0.002777*	*0.002777*	0.002778	0.002799	0.002820	0.002840	0.002851	0.002872	0.002884	0.002896	0.002901	0.002921	0.002927	0.002951	0.002978	0.003022	0.003045	0.003077	0.003130
	p_B	*0.0*	*2.411*	4.885	7.309	9.570	11.84	13.92	15.84	17.50	18.88	19.95	20.82	21.45	22.35	22.92	23.38	23.56	23.76	23.85
0.07	p_W	*21.99*	*21.93*	21.78	21.65	21.53	21.41	21.29	21.19	21.10	21.02	20.95	20.90	20.85	20.77	20.71	20.66	20.61	20.55	20.52
	p_D	*0.004243*	*0.004243*	0.004304	0.004331	0.004360	0.004384	0.004414	0.004423	0.004442	0.004458	0.004482	0.004485	0.004510	0.004550	0.004596	0.004623	0.004697	0.004767	0.004821
	p_B	*0.0*	*2.441*	4.998	7.475	9.773	12.02	14.07	15.96	17.55	18.87	19.90	20.72	21.33	22.24	22.83	23.29	23.51	23.74	23.85
0.09	p_W	*21.30*	*21.24*	21.09	20.96	20.83	20.71	20.61	20.50	20.42	20.34	20.28	20.22	20.17	20.09	20.02	19.95	19.90	19.85	19.80
	p_D	*0.006107*	*0.006107*	0.006192	0.006234	0.006274	0.006310	0.006330	0.006368	0.006391	0.006414	0.006424	0.006465	0.006478	0.006530	0.006587	0.006688	0.006747	0.006816	0.006926
	p_B	*0.0*	*2.482*	5.093	7.607	9.924	12.14	14.14	15.98	17.52	18.77	19.75	20.55	21.15	22.05	22.65	23.14	23.39	23.63	23.79
0.11	p_W	*20.55*	*20.49*	20.33	20.20	20.08	19.97	19.86	19.76	19.68	19.61	19.54	19.49	19.45	19.35	19.27	19.21	19.15	19.07	19.02
	p_D	*0.008440*	*0.008440*	0.008558	0.008610	0.008659	0.008700	0.008752	0.008767	0.008797	0.008822	0.008867	0.008871	0.008917	0.008995	0.009093	0.009144	0.009273	0.009420	0.009536
	p_B	*0.0*	*2.522*	5.175	7.704	10.02	12.19	14.14	15.92	17.39	18.57	19.52	20.29	20.88	21.80	22.43	22.90	23.20	23.47	23.66
0.13	p_W	*19.74*	*19.68*	19.52	19.39	19.28	19.17	19.07	18.97	18.89	18.82	18.76	18.70	18.66	18.57	18.50	18.40	18.34	18.28	18.21
	p_D	*0.01133*	*0.01133*	0.01148	0.01154	0.01160	0.01165	0.01167	0.01172	0.01176	0.01179	0.01181	0.01187	0.01190	0.01199	0.01207	0.01226	0.01238	0.01250	0.01267
	p_B	*0.0*	*2.556*	5.229	7.753	10.05	12.17	14.05	15.77	17.17	18.29	19.20	19.96	20.54	21.46	22.10	22.61	22.95	23.21	23.43
0.15	p_W	*18.88*	*18.83*	18.67	18.55	18.44	18.33	18.23	18.15	18.07	18.01	17.94	17.89	17.84	17.75	17.65	17.59	17.52	17.43	17.36
	p_D	*0.01487*	*0.01487*	0.01504	0.01510	0.01516	0.01520	0.01528	0.01529	0.01533	0.01536	0.01543	0.01543	0.01549	0.01562	0.01580	0.01588	0.01605	0.01630	0.01651
	p_B	*0.0*	*2.577*	5.248	7.746	10.00	12.06	13.89	15.53	16.86	17.92	18.82	19.54	20.13	21.06	21.74	22.22	22.59	22.89	23.15
0.17	p_W	*17.99*	*17.94*	17.79	17.67	17.56	17.46	17.38	17.29	17.22	17.16	17.11	17.04	16.99	16.90	16.83	16.73	16.65	16.59	16.52
	p_D	*0.01915*	*0.01915*	0.01933	0.01940	0.01946	0.01952	0.01952	0.01958	0.01962	0.01967	0.01967	0.01977	0.01982	0.01995	0.02004	0.02031	0.02054	0.02071	0.02092
	p_B	*0.0*	*2.580*	5.226	7.680	9.891	11.87	13.63	15.19	16.46	17.48	18.34	19.07	19.65	20.58	21.26	21.78	22.19	22.48	22.74
0.19	p_W	*17.07*	*17.03*	16.88	16.78	16.68	16.59	16.50	16.42	16.36	16.30	16.23	16.19	16.14	16.05	15.94	15.88	15.80	15.71	15.62
	p_D	*0.02427*	*0.02427*	0.02447	0.02452	0.02456	0.02458	0.02466	0.02467	0.02470	0.02471	0.02481	0.02480	0.02487	0.02501	0.02531	0.02545	0.02565	0.02598	0.02635
	p_B	*0.0*	*2.562*	5.161	7.551	9.696	11.59	13.30	14.78	15.97	16.95	17.81	18.50	19.09	20.03	20.75	21.26	21.67	22.00	22.30
0.21	p_W	*16.15*	*16.10*	15.97	15.87	15.78	15.69	15.62	15.55	15.48	15.42	15.38	15.32	15.27	15.17	15.10	15.01	14.92	14.85	14.80
	p_D	*0.03034*	*0.03034*	0.03051	0.03054	0.03057	0.03062	0.03057	0.03061	0.03063	0.03068	0.03065	0.03078	0.03085	0.03106	0.03112	0.03142	0.03178	0.03203	0.03217
	p_B	*0.0*	*2.523*	5.050	7.360	9.429	11.24	12.88	14.28	15.41	16.37	17.19	17.89	18.48	19.43	20.13	20.67	21.11	21.43	21.70
0.23	p_W	*15.22*	*15.17*	15.05	14.96	14.88	14.81	14.73	14.67	14.61	14.56	14.49	14.45	14.41	14.33	14.22	14.14	14.06	13.97	
	p_D	*0.03743*	*0.03743*	0.03757	0.03757	0.03756	0.03749	0.03754	0.03752	0.03753	0.03752	0.03765	0.03763	0.03768	0.03777	0.03817	0.03846	0.03870	0.03914	
	p_B	*0.0*	*2.462*	4.896	7.115	9.095	10.81	12.40	13.72	14.80	15.72	16.55	17.22	17.81	18.75	19.50	20.05	20.47	20.83	
0.25	p_W	*14.29*	*14.25*	14.15	14.07	13.99	13.91	13.86	13.79	13.74	13.69	13.65	13.60	13.55	13.44	13.37	13.29	13.19	13.12	
	p_D	*0.04562*	*0.04562*	0.04570	0.04563	0.04556	0.04558	0.04547	0.04545	0.04542	0.04547	0.04536	0.04547	0.04555	0.04592	0.04604	0.04632	0.04678	0.04708	
	p_B	*0.0*	*2.380*	4.704	6.816	8.700	10.35	11.85	13.10	14.12	15.05	15.83	16.51	17.10	18.07	18.79	19.35	19.79	20.14	
0.27	p_W	*13.39*	*13.35*	13.26	13.18	13.11	13.06	12.99	12.94	12.89	12.84	12.78	12.74	12.69	12.63	12.54	12.45	12.40		
	p_D	*0.05495*	*0.05495*	0.05496	0.05486	0.05474	0.05457	0.05453	0.05445	0.05442	0.05434	0.05451	0.05452	0.05461	0.05455	0.05486	0.05517	0.05531		
	p_B	*0.0*	*2.282*	4.481	6.485	8.271	9.820	11.27	12.44	13.43	14.32	15.12	15.78	16.37	17.29	18.03	18.61	19.02		

0.29	p_W	*12.51*	*12.47*	12.39	12.32	12.27	12.20	12.15	12.10	12.05	12.00	11.97	11.92	11.89	11.77	11.68	11.56	11.37
	p_D	*0.06543*	*0.06543*	0.06538	0.06517	0.06493	0.06488	0.06469	0.06460	0.06452	0.06457	0.06438	0.06439	0.06437	0.06487	0.06531	0.06607	0.06771
	p_B	*0.0*	*2.171*	4.241	6.126	7.802	9.288	10.66	11.77	12.71	13.61	14.36	15.01	15.58	16.55	17.30	17.93	18.47
0.31	p_W	*11.67*	*11.63*	11.56	11.50	11.44	11.39	11.34	11.29	11.24	11.21	11.14	11.09	11.02	10.93	10.84	10.79	
	p_D	*0.07698*	*0.07698*	0.07683	0.07658	0.07643	0.07613	0.07599	0.07585	0.07578	0.07559	0.07580	0.07595	0.07630	0.07657	0.07701	0.07702	
	p_B	*0.0*	*2.054*	3.988	5.761	7.346	8.740	10.04	11.09	12.01	12.87	13.63	14.29	14.88	15.82	16.56	17.13	
0.33	p_W	*10.87*	*10.84*	10.77	10.71	10.66	10.60	10.55	10.50	10.45	10.38	10.34	10.30	10.28	10.22	10.21		
	p_D	*0.08946*	*0.08946*	0.08934	0.08908	0.08872	0.08863	0.08844	0.08836	0.08834	0.08859	0.08851	0.08851	0.08825	0.08806	0.08747		
	p_B	*0.0*	*1.938*	3.749	5.415	6.890	8.231	9.447	10.46	11.35	12.21	12.93	13.57	14.10	15.00	15.66		
0.35	p_W	*10.13*	*10.10*	10.03	9.972	9.909	9.860	9.809	9.766	9.726	9.712	9.685	9.668	9.633	9.574	9.445		
	p_D	*0.1026*	*0.1026*	0.1025	0.1022	0.1022	0.1019	0.1018	0.1016	0.1014	0.1008	0.1005	0.1001	0.1000	.09982	0.1009		
	p_B	*0.0*	*1.832*	3.531	5.095	6.497	7.763	8.888	9.855	10.71	11.48	22.54	12.77	13.29	14.18	14.94		

strength of i−j intermolecular interaction in terms of chemical potential.

$$\mu_{ij}^{E} = N(\partial\mu_i^{E}/\partial n_j) = (1 - x_j)\,(\partial\mu_i^{E}/\partial x_j) - \sum{}' x_k(\partial\mu_i^{E}/\partial x_k) \tag{4}$$

The summation $\sum'$ runs from 1 to $N - 1$, except for j, where N is the number of components, and N refers generally to the solvent. Due to the stability criterion regarding chemical potential, a negative value of μ_{ij}^{E} implies that the addition of the j-th component brings about a more favorable situation in terms of chemical potential for the existing i-th component. Hence, the i−j interaction is said to be attractive (favorable) in terms of chemical potential. Conversely, if $\mu_{ij}^{E} > 0$, the i−j interaction is repulsive. This quantity, eq 4, is equivalent to the preferential binding coefficient used by Timasheff and others.[18] It is useful in understanding net interactions in solutions. However, due to the entropy−enthalpy compensation generally observed in aqueous solutions,[11] details of the mixing scheme or the solution "structure" are much more conspicuous in enthalpic and entropic solute−solute interactions; see eqs 5 and 6. μ_{ij}^{E} is the second derivative of G, which provides

$$H_{ij}^{E} = N(\partial H_i^{E}/\partial n_j) \tag{5}$$

$$S_{ij}^{E} = N(\partial S_i^{E}/\partial n_j) \tag{6}$$

information about the net interaction in terms of chemical potential, that dictates the fate of an equilibrium system. On the other hand, H_{ij}^{E} or S_{ij}^{E} are the third derivatives, and thus any singular behavior in a thermodynamic property is more conspicuous in H_{ij}^{E} and S_{ij}^{E}.

The values of μ_{BD}^{E} and those of μ_{BB}^{E} calculated by eq 4 are plotted in Figure 3 (see also Table 4). The uncertainty in μ_{BD}^{E} is ± 0.03 kJ mol^{-1} as mentioned in Appendix I. That for μ_{BB}^{E} should be about the same if not better. Figure 3a indicates that TBA−TBA interaction in terms of chemical potential is attractive in the entire region studied; i.e., $\mu_{BB}^{E} < 0$. In the binary TBA−H_2O, the TBA−TBA interaction was found to be net attractive due to a stronger entropic attraction than the enthalpic repulsion. For $x_B < 0.0525$, μ_{BB}^{E} become more negative as x_D increases; thus, addition of DMSO enhances the TBA−TBA attraction. For $x_B > 0.065$, on the other hand, μ_{BB}^{E} increases slightly, which implies that the TBA−TBA attraction is retarded by further addition of DMSO. The threshold value of x_B of these two different behaviors matches that of the mixing scheme boundary between I and II for the binary TBA−H_2O. Thus, the effect of DMSO on the TBA−TBA interaction depends qualitatively on whether the aqueous solution in question is in mixing scheme I or II. Figure 3b shows that DMSO−TBA interactions are more intricate. The initial decrease in μ_{BD}^{E} as a function of x_B is not observed for higher values of x_D, certainly not for $x_D > 0.3$, which is beyond the I−II boundary in the binary DMSO−H_2O.

For a better understanding of the known cryoprotective and toxic effect of DMSO on living cells,[20,21] the net interactions (in chemical potential) of DMSO on a hydrophobic moiety (TBA) (the information contained in Figure 3) may be of some importance. Since it was originally discovered by Lovestock and Bishop[17] that DMSO protects red cells against injuries induced by freeze−thaw cycles, this solute has been commonly used as a cryoprotectant for macromolecules, organelles, cells, and tissues.[19] However, DMSO in concentrations high enough to protect against injuries at subzero temperatures may be harmful to nonfrozen cells. Arakawa et al.[20] suggested that this

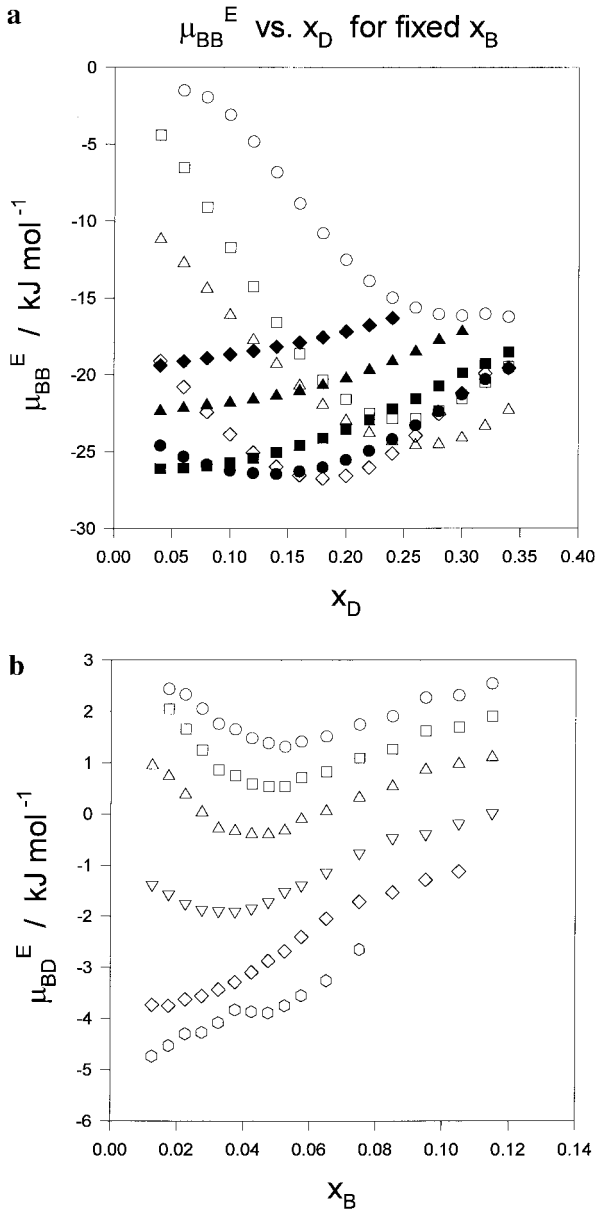

Figure 3. (a) TBA−TBA interactions in terms of excess chemical potential, μ_{BB}^{E}, at 24.95 °C as function of x_D for selected values of x_B: (○) 0.0125; (□) 0.0225; (△) 0.0325; (◇) 0.0425; (●) 0.0525; (■) 0.065; (▲) 0.085; (◆) 0.105. (b) TBA−DMSO interactions in terms of chemical potential, μ_{BD}^{E}, at 24.95 °C as a function of x_B for selected values of x_D: (○) 0.04; (□) 0.08; (△) 0.12; (▽) 0.16; (◇) 0.24; (⬡) 0.34.

toxicity was related to a general destabilizing effect of DMSO on protein conformations[22] and that the mechanism for the destabilization was hydrophobic binding of DMSO to nonpolar areas on the protein surfaces. Neutron diffraction studies by Lehman and Stanford have offered some support to this suggestion.[23] However, as discussed above the μ-wise interactions of DMSO with a predominantly hydrophobic solute like TBA are weak and in fact repulsive for $x_D < 0.12$, i.e., $\mu_{DB}^{E} > 0$, as shown in Figure 3b. This concentration range corresponds to less than 35 wt % and encompasses concentrations typically used in freeze preservation protocols.[19,21] Thus, although DMSO in binary aqueous solution appears to be a hydrophobic solute,[6,24] results from the present and a previous[25] investigation of a ternary system do not support the suggestion that binding to nonpolar moieties of biopolymers is the basis for the observed effect.

Figure 3a shows another example of complexity of the effect of DMSO on hydrophobic moieties. In the water-rich region, μ_{BB}^{E} becomes more negative with increasing DMSO concentration, and thus DMSO acts to enhance attractive (hydrophobic) interaction among TBA molecules. At higher concentrations of TBA, this trend is reversed. Thus, it seems reasonable to conclude that discussions of mechanisms underlying effects of DMSO on protein conformations will require a more detailed analysis of protein−solute interactions, not only in terms of free energy but also in those of constituent enthalpy and entropy. More importantly, the composition range of solutes must be specified clearly in such a discussion. Generalized interpretations on the propensity of DMSO to weaken hydrophobic interactions[26] or to be preferentially bound to nonpolar surfaces[20] without specifying concentration ranges of solutes are unlikely to give a realistic picture.

In the context of the effect of organic solute on the "hydrophobic interactions" in mixed aqueous solvents, the following two sets of investigations are worth noting. Yaacobi and Ben-Naim measured solubilities of methane and ethane in mixed aqueous solvent of ethanol[30] and dioxane.[31] A measure of "hydrophobic interaction" between two CH_4 molecules referenced to that of CH_3-CH_3 in solution was evaluated.[36] The resulting measure in Gibbs function showed maxima at about 0.05 of ethanol mole fraction (30 °C), and 0.03 (10 °C), and minima at 0.15 (30 °C) and 0.2 (10 °C) for ethanol−H_2O.[30] For dioxane−H_2O, however, there was no maximum but the minimum at about 0.1 mole fraction of dioxane at 10 and 25 °C. They thus noted a change in behavior of the "hydrophobic interaction" at these extrema. Oakenfull and Fenwick[32−34] determined the ion-pair association constant and hence the Gibbs energy change of long-chain decyltrimethylammonium carboxylates in aqueous mixed solvents. By changing systematically the chain length of the alkyl group, they devised a method of evaluating a measure of the "hydrophobic interaction" between intermolecular $-CH_2-$ groups in terms of the Gibbs energy. The resulting measures pass through minima (maximum hydrophobic interactions) with increasing mole fractions of the organic component in all but dioxane−H_2O. At 25 °C the minima occurred at a mole fraction of about 0.03 for *tert*-butyl alcohol, 0.25 for DMSO,[34] and 0.1 for ethanol.[32] Thus, they clearly noted that the behavior of "hydrophobic interaction" depends crucially on the mole fraction range of the organic component of mixed aqueous solvents. The loci of minima are rather close to the boundaries of mixing schemes I and II from our previous works in the respective binary aqueous solutions: 0.05 for *tert*-butyl alcohol,[1−5] 0.28 for DMSO,[6] and 0.125 for ethanol.[35] We discuss below in detail the effect of a third component on the boundary between mixing schemes I and II.

Partial Molar Enthalpies and Entropies. Figure 4 shows the plots of TS_{BB}^{E} and TS_{BD}^{E}, together with those of H_{BB}^{E} and H_{BD}^{E},[16] at 26.90 °C. The uncertainty in H_{BB}^{E} and TS_{BB}^{E} is about 20 kJ mol^{-1} while that for H_{BD}^{E} and TS_{BD}^{E} is ± 5 kJ mol^{-1}. In comparison with Figure 3, H_{ij}^{E} and TS_{ij}^{E} are an order of magnitude larger than μ_{ij}^{E}, and strongly compensating with each other. As discussed before,[8,16] the anomalous behaviors of H_{ij}^{E} and TS_{ij}^{E} shown in Figure 4 suggest a qualitative change in the thermodynamic properties of the solution, the transition of the mixing scheme. Such anomalous behaviors are apparent in the third derivatives (Figure 4) but not so clearly in the second derivative (Figure 3). The solid line from $x_B = 0$ to point *X* in Figure 4 represents the thermodynamic behavior in mixing scheme I, which is characterized by strong TBA−TBA and TBA−DMSO repulsion in terms of enthalpy but almost equally

TABLE 4: μ_{BD}^E and μ_{DB}^E in kJ mol (Consistency Check, See Text)

		x_B																
x_D		0.0125	0.0175	0.0225	0.0275	0.0325	0.0375	0.0425	0.0475	0.0525	0.0575	0.065	0.075	0.085	0.095	0.105	0.115
0.04	μ_{BD}^E		2.41	2.30	2.00	1.73	1.60	1.43	1.32	1.28	1.35	1.46	1.70	1.87	2.21	2.26	2.50
	μ_{DB}^E		2.43	2.33	2.05	1.76	1.65	1.47	1.37	1.31	1.40	1.51	1.75	1.91	2.27	2.32	2.54
0.06	μ_{BD}^E	2.65	2.69	2.28	1.86	1.48	1.27	1.08	1.02	0.98	1.07	1.23	1.48	1.59	1.92	2.08	2.31
	μ_{DB}^E	2.65	2.70	2.29	1.87	1.50	1.29	1.10	1.03	1.02	1.08	1.24	1.50	1.62	1.93	2.09	2.34
0.08	μ_{BD}^E	2.09	2.05	1.65	1.22	0.86	0.73	0.58	0.51	0.54	0.69	0.82	1.08	1.27	1.61	1.68	1.91
	μ_{DB}^E	2.07	2.05	1.65	1.24	0.86	0.74	0.59	0.53	0.53	0.71	0.83	1.09	1.26	1.63	1.70	1.91
0.10	μ_{BD}^E	1.63	1.45	1.03	0.68	0.34	0.17	0.063	0.069	0.11	0.25	0.45	0.76	0.88	1.15	1.38	1.60
	μ_{DB}^E	1.61	1.44	1.03	0.68	0.36	0.18	0.070	0.065	0.13	0.24	0.45	0.76	0.89	1.14	1.38	1.61
0.12	μ_{BD}^E	0.97	0.74	0.38	0.021	−0.27	−0.34	−0.40	−0.41	−0.31	−0.11	0.049	0.31	0.55	0.85	0.96	1.10
	μ_{DB}^E	0.94	0.73	0.38	0.031	−0.28	−0.33	−0.40	−0.40	−0.32	−0.10	0.051	0.32	0.54	0.86	0.97	1.10
0.14	μ_{BD}^E	0.23	−0.020	−0.34	−0.57	−0.79	−0.89	−0.91	−0.84	−0.73	−0.58	−0.34	0.012	0.19	0.35	0.61	0.80
	μ_{DB}^E	0.20	−0.030	−0.35	−0.59	−0.78	−0.88	−0.90	−0.85	−0.72	−0.58	−0.34	0.007	0.20	0.35	0.60	0.81
0.16	μ_{BD}^E	−0.56	−0.77	−0.99	−1.23	−1.41	−1.40	−1.35	−1.30	−1.14	−0.91	−0.70	−0.47	−0.20	0.084	0.24	0.27
	μ_{DB}^E	−0.58	−0.78	−1.00	−1.22	−1.42	−1.40	−1.35	−1.29	−1.16	−0.90	−0.70	−0.46	−0.22	0.085	0.25	0.28
0.18	μ_{BD}^E	−1.35	−1.55	−1.75	−1.85	−1.90	−1.91	−1.85	−1.70	−1.54	−1.39	−1.13	−0.75	−0.48	−0.40	−0.18	0.027
	μ_{DB}^E	−1.37	−1.56	−1.75	−1.86	−1.89	−1.91	−1.84	−1.71	−1.52	−1.39	−1.14	−0.76	−0.47	−0.39	−0.18	0.021
0.20	μ_{BD}^E	−2.19	−2.32	−2.36	−2.47	−2.50	−2.42	−2.28	−2.16	−1.95	−1.69	−1.41	−1.18	−0.95	−0.67	−0.49	−0.54
	μ_{DB}^E	−2.21	−2.33	−2.37	−2.46	−2.51	−2.42	−2.28	−2.14	−1.97	−1.68	−1.42	−1.17	−0.96	−0.68	−0.48	−0.52
0.22	μ_{BD}^E	−2.94	−3.03	−3.09	−3.09	−2.94	−2.85	−2.72	−2.48	−2.25	−2.10	−1.87	−1.50	−1.12	−0.99	−0.82	
	μ_{DB}^E	−2.97	−3.04	−3.09	−3.10	−2.94	−2.85	−2.72	−2.50	−2.23	−2.09	−1.87	−1.51	−1.12	−0.99	−0.82	
0.24	μ_{BD}^E	−3.70	−3.73	−3.60	−3.56	−3.43	−3.28	−3.09	−2.89	−2.67	−2.40	−2.03	−1.72	−1.53	−1.28	−1.12	
	μ_{DB}^E	−3.73	−3.75	−3.62	−3.55	−3.43	−3.28	−3.09	−2.87	−2.68	−2.40	−2.04	−1.71	−1.53	−1.28	−1.12	
0.26	μ_{BD}^E	−4.29	−4.22	−4.16	−4.10	−3.80	−3.62	−3.45	−3.11	−2.79	−2.60	−2.42	−2.17	−1.83	−1.66		
	μ_{DB}^E	−4.31	−4.23	−4.15	−4.11	−3.80	−3.62	−3.45	−3.13	−2.79	−2.60	−2.41	−2.18	−1.83	−1.65		
0.28	μ_{BD}^E	−4.78	−4.76	−4.53	−4.36	−4.09	−3.87	−3.64	−3.37	−3.20	−2.99	−2.59	−2.11	−1.73	−1.08		
	μ_{DB}^E	−4.80	−4.77	−4.55	−4.36	−4.09	−3.87	−3.65	−3.36	−3.20	−2.98	−2.60	−2.11	−1.74	−1.12		
0.30	μ_{BD}^E	−5.10	−4.89	−4.70	−4.61	−4.25	−4.00	−3.86	−3.50	−3.10	−2.76	−2.47	−2.22	−2.13			
	μ_{DB}^E	−5.13	−4.91	−4.70	−4.62	−4.26	−4.01	−3.85	−3.52	−3.11	−2.78	−2.46	−2.22	−2.12			
0.32	μ_{BD}^E	−4.98	−4.91	−4.70	−4.50	−4.19	−3.88	−3.61	−3.30	−3.15	−3.08	−3.02	−2.94				
	μ_{DB}^E	−5.01	−4.92	−4.72	−4.51	−4.20	−3.89	−3.64	−3.29	−3.15	−3.05	−3.02	−2.92				
0.34	μ_{BD}^E	−4.70	−4.50	−4.29	−4.26	−4.08	−3.83	−3.89	−3.89	−3.76	−3.54	−3.25	−2.62				
	μ_{DB}^E	−4.73	−4.53	−4.30	−4.27	−4.08	−3.83	−3.86	−3.89	−3.74	−3.55	−3.26	−2.64				

strong entropic attraction. Small differences between the two give net attraction in terms of chemical potential for TBA−TBA and net TBA−DMSO repulsion. These strong interactions in enthalpy and entropy are operative via the hydrogen bond network of solvent H_2O. Point X in Figure 4 is regarded as the beginning of the transition to mixing scheme II. If the notion that the hydrogen bond strength in liquid water is widely fluctuating is accepted,[27] then those hydrogen bonds at the strongest end of spectrum reach the percolation threshold at *X*, so that the connectivity through those strongest hydrogen bonds is no longer present. As the concentration of solute increases, the hydrogen bond strength distribution is skewed progressively to the weak side. At point *Y*, the "weakest" hydrogen bond probability reaches the percolation threshold and as a result no trace of hydrogen bond connectivity exists any longer. The solution then consists of two kinds of clusters rich in each component, i.e., mixing scheme II, in which both enthalpic and entropic interactions become very weak. Since there is no bond-percolation, these interactions are operative locally within the clusters. Thus, the transition from mixing scheme I to mixing scheme II occurs in the composition range from *X* to *Y* with the midpoint *M*. Figure 4 indicates such transition region move toward lower concentrations with increasing DMSO concentration. This supports the view that TBA and DMSO have a similar effect on the hydrogen bond network of solvent water. With DMSO already modifying H_2O, a smaller amount of TBA is required to drive the system to mixing scheme II.

Partial Molar Volumes and General Discussion. Figure 5 shows typical data for the partial molar volume of DMSO, V_D. At $x_B = 0.0187$, V_D still shows an initial decrease, indicative of mixing scheme I behavior.[6−8] Smooth curves are drawn for all the series of different TBA compositions and are reproduced in Figure 6. The initial decrease in V_D as x_D increases from zero, which is characteristic of mixing scheme I,[6,14] diminishes as the TBA content increases, and for $x_B > 0.0581$, beyond the transition in binary TBA−H_2O, there is no sign of mixing scheme I behavior in V_D. This also supports the view that TBA and DMSO modifies the hydrogen bond network in the same way. The composition derivative, V_{DD}^E was calculated for $x_B^0 = 0.01870$ as

$$V_{DD}^E = N(\partial V_D^E/\partial n_D) = N(\partial V_D/\partial n_D) \qquad (7)$$

Since there is no stability criterion for volume, V_{DD}^E, a third derivative, indicates only the effect of the incoming DMSO on the partial molar volume of the existing DMSO. Figure 7 shows the plots of V_{DD}^E. Instead of a sharp peak seen in similar plots for 2-butoxyethanol−H_2O,[14] a broad volcano with a flat top is apparent, just as seen for binary DMSO−H_2O.[6] This can be interpreted in the same way as H_{ij}^E and S_{ij}^E (Figure 3). Thus, the transition in the mixing schemes takes place from point *X* to point *Y* with a nominal midpoint *M* as shown in Figure 7. This interpretation is in no way unequivocal within the data shown in Figure 7 alone but may be justified by the behaviors of H_{ij}^E and S_{ij}^E (Figure 4).

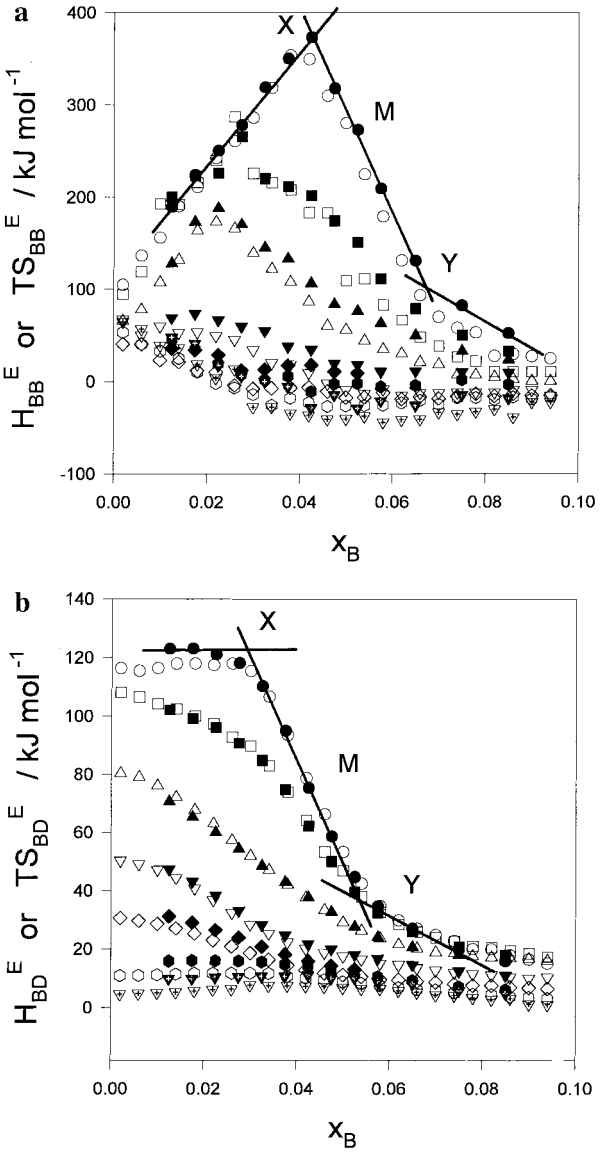

Figure 4. (a) TBA−TBA interaction in terms of enthalpy, H_{BB}^E (open symbols), and entropy, TS_{BB}^E (filled symbols), at 26.90 °C as a function of x_B for selected values of x_D: (○) 0.0; (□) 0.0478; (△) 0.1031; (▽) 0.1999; (◇) 0.2341; (⬡) 0.2735; (plus in triangle) 0.3540. (b) TBA−DMSO interaction in terms of enthalpy, H_{BD}^E (open symbols), and entropy, TS_{BD}^E (filled symbols), at 26.90 °C as a function of x_B for selected values of x_D: (○) 0.0239; (□) 0.0478; (△) 0.1031; (▽) 0.1999; (◇) 0.2341; (⬡) 0.2735; (plus in triangle) 0.3540.

The loci of points *X*, *Y*, and *M* from the plots of TS_{ij}^E shown in Figure 4 (those[16] from H_{ij}^E are almost the same as those from TS_{ij}^E) and that from V_{DD}^E (Figure 7) are plotted in Figure 8. It is striking that the loci of *X*, *Y*, and *M* fall approximately on almost parallel straight lines. This suggests that the effects of DMSO and TBA on solvent water are *additive*. When DMSO solutes are present, a *proportionally* lesser amount of TBA is required to drive the system to mixing scheme II and vice versa. Thus, the nature of interaction toward solvent water is the same, despite an apparent difference in the balance of hydrophobic/hydrophilic moieties; on one hand, *tert*-butyl- vs −OH groups, with two methyl- vs one sulfoxide on the other. This difference was sought previously[6] to be the source of a difference in the partial molar enthalpy/entropy behavior at the infinite dilution. For TBA−H_2O,[4] the enthalpy gain was smaller than the entropy loss as the first TBA settles in an aqueous environment, while the enthalpy gain was larger for DMSO−H_2O.[6] Nevertheless, the information contained in Figure 8 suggests that the effect of each solute on H_2O to break up the percolation nature of H_2O is the same and is additive. There is, however, evidence

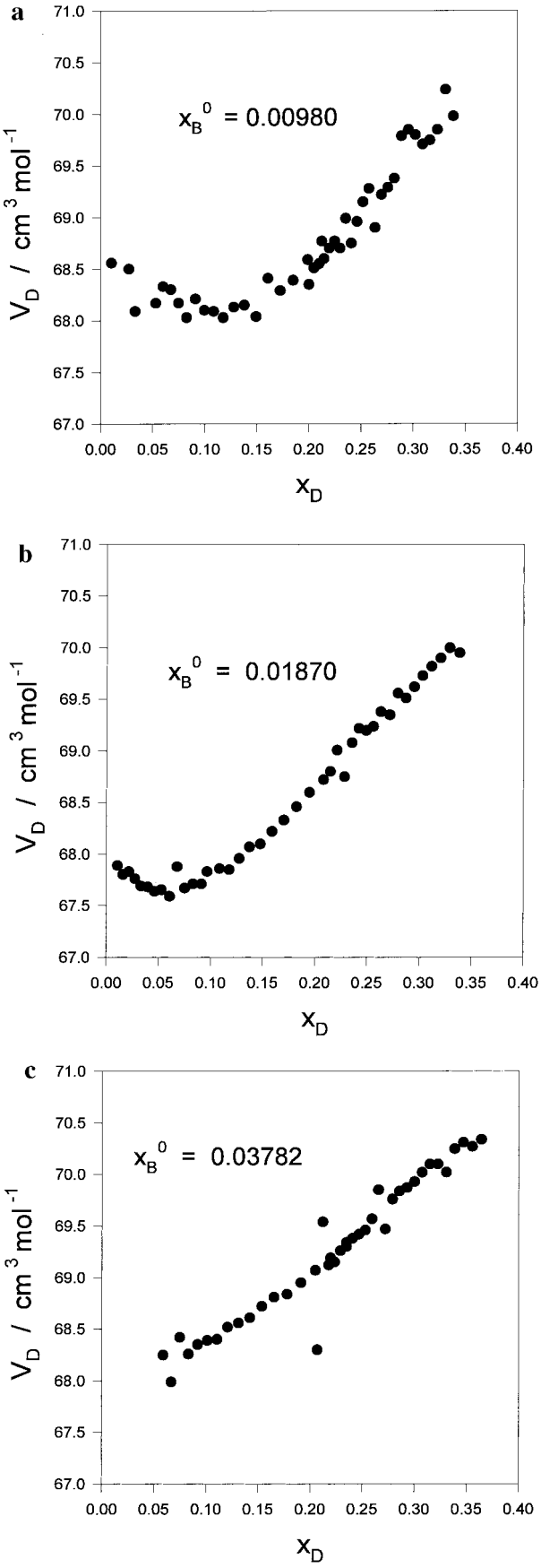

Figure 5. Partial molar volume of DMSO, V_D, at 25 °C as a function of x_D for selected intial values of x_B^0: (a) $x_B^0 = 0.00980$, (b) $x_B^0 = 0.01870$, and (c) $x_B^0 = 0.03782$.

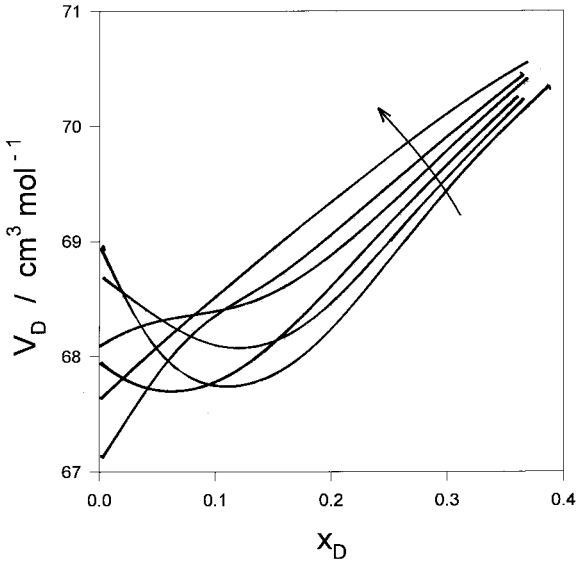

Figure 6. Smoothed garph of partial molar volumes of DMSO, V_D, at 25 °C as a function of x_D for selected initial values of x_B^0. Along the direction of arrow, $x_B^0 = 0$, 0.00980, 0.01870, 0.0298, 0.03782, and 0.0900.

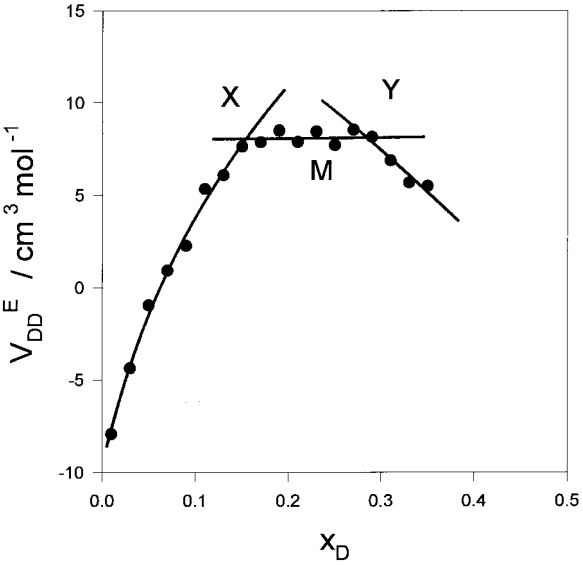

Figure 7. DMSO−DMSO interaction in terms of volume, V_{DD}^E. See text, eq 7, for $x_B^0 = 0.01870$.

in the pair correlation function between S atoms determined by a recent careful X-ray scattering measurements that in mixing scheme I in binary DMSO−H_2O, DMSO molecules tend to form dimers, tetramers, etc., via S═O dipoles.[28] As a result, hydrophilic parts may be hidden inside these oligomers, whose surfaces are covered with methyl groups, acting as a strong hydrophobic solute. However, this alone does not yet explain why DMSO and TBA work in an additive manner.

Acknowledgment. This work was supported by the NSERC of Canada and a NATO Collaborative Research Project.

Appendix I. Numerical Evaluation of Partial Pressures

The pressures shown in Table 1 were determined within ±0.001 Torr as long as the temperature of the cell was controlled within ±0.001 °C, which was the case during the determination of one data point. The day to day fluctuation of the bath controlled at 24.95 °C amounted to about ±0.005 °C. By

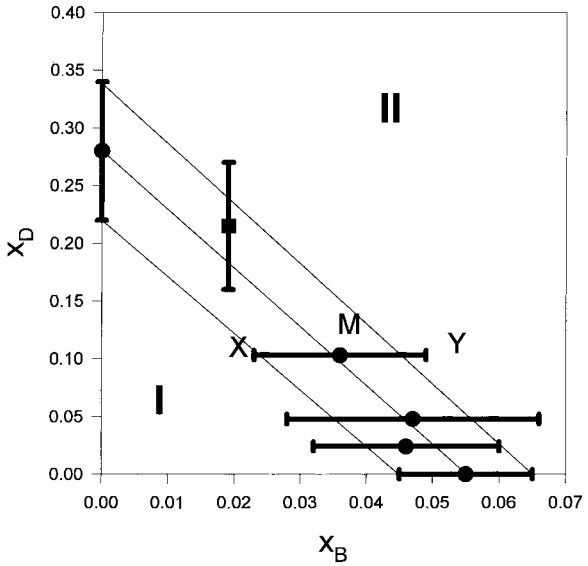

Figure 8. Mixing scheme boundary (I to II) in ternary system TBA−DMSO−H_2O at 25 °C. *X* is the onset of transition from mixing scheme I to II, and *Y* is the end point. *M* is the midpoint, i.e., the nominal transition point.

interpolation, the smoothed vapor pressures are given in Table 2. The uncertainty was estimated as ±0.01 Torr, which is larger than that expected for the temperature variation of ±0.005 °C. Hence the temperature was regarded as being constant within experimental uncertainty.

Smoothed values of p given at a grid of (x_B , x_D) in Table 2 are the starting point of our data analysis. Consider the calculation matrix (m, n)

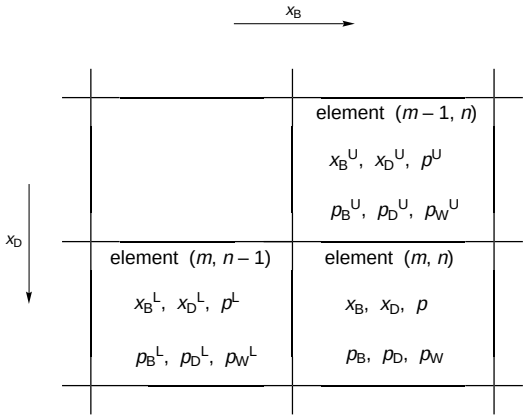

which is of the same form as Table 2. The first element (1, 1) contains all the data pertaining to pure water, i.e., $x_D = 0$, $x_B = 0$, $p_D = 0$, $p_B = 0$, and $p_W = p$. The first column (m, 1) is for the binary mixtures of DMSO−H_2O, and the first row (1, n) is for TBA−H_2O. In a given element (m, n), the values of x_D, x_B, and p are known. Our goal is to evaluate the partial pressures, p_B , p_D, and p_W in this element. Suppose that the "up" element immediately above in the same column (m −1, n) and the "left"-element immediately left in the same row (m, n − 1) are already solved and all the partial pressures are known. All the data in the "up" element in the same column (m − 1, n) are designated with superscript U, while those of the "left" element with L. Note that $x_B = x_B^U$ and $x_D = x_D^L$, being in the same column and row, respectively, as the element of interest. Next we assume that the change in x_D from the "up" element down to the element of interest is sufficiently small and that the Gibbs−Duhem relation holds for the resulting

TABLE 5: Density of TBA−DMSO−H_2O Solutions at 26.90 ± 0.005 °C (Error in d ± 0.00001 g cm^{-3})

x_D	x_B	d/g cm^{-3}	x_D	x_B	d/g cm^{-1}	x_D	x_B	d/g cm^{-3}	x_D	x_B	d/g cm^{-1}
					$x_B^0 = 0$						
0	0	0.99647	0.00476	0	0.99833	0.22893	0	1.07603	0.23567	0	1.07727
0.00976	0	1.00088	0.01484	0	1.00346	0.24272	0	1.07854	0.24985	0	1.07974
0.02016	0	1.00610	0.02569	0	1.00880	0.25725	0	1.08091	0.26470	0	1.08202
0.03130	0	1.01149	0.03725	0	1.01431	0.27240	0	1.08312	0.28051	0	1.08421
0.04340	0	1.01717	0.04972	0	1.02006	0.28863	0	1.08524	0.29712	0	1.08629
0.05623	0	1.02296	0.06302	0	1.02592	0.30576	0	1.08723	0.31471	0	1.08814
0.07010	0	1.02891	0.07757	0	1.03198	0.32394	0	1.08901	0.33342	0	1.08984
0.08517	0	1.03503	0.09324	0	1.03816	0.34327	0	1.09064	0.35331	0	1.09138
0.10165	0	1.04133	0.11035	0	1.04448	0.36380	0	1.09208	0.37469	0	1.09275
0.11945	0	1.04767	0.12892	0	1.05109	0.38576	0	1.09336	0.39738	0	1.09395
0.13894	0	1.05433	0.14937	0	1.05747	0.41131	0	1.09456	0.42421	0	1.09505
0.16037	0	1.06048	0.17391	0	1.06375	0.43691	0	1.09548	0.45006	0	1.09586
0.18642	0	1.06652	0.19958	0	1.06982	0.46368	0	1.09619	0.47786	0	1.09649
0.21339	0	1.07280	0.22787	0	1.07546						
0.24273	0	1.07838	0.25855	0	1.08099						
0.18642	0	1.06652	0.19958	0	1.06982						
0.21339	0	1.07280	0.22787	0	1.07546						
0.24273	0	1.07838	0.25855	0	1.08099						
					$x_B^0 = 0.00980$						
0	0.00980	0.99008	0.00512	0.00975	0.99598	0.19552	0.00788	1.06470	0.20021	0.00784	1.06578
0.01035	0.00970	0.99867	0.01583	0.00964	0.99954	0.20493	0.00779	1.06683	0.20978	0.00774	1.06787
0.02141	0.00959	1.00412	0.02723	0.00953	1.00688	0.21476	0.00770	1.06891	0.21976	0.00765	1.06992
0.03328	0.00947	1.00981	0.03956	0.00941	1.01197	0.22488	0.00760	1.07092	0.23011	0.00754	1.07193
0.04619	0.00935	1.01562	0.05288	0.00928	1.01856	0.23544	0.00749	1.07288	0.24087	0.00744	1.07389
0.05991	0.00921	1.02151	0.06726	0.00914	1.02451	0.24639	0.00739	1.07484	0.25209	0.00733	1.07578
0.07476	0.00907	1.02750	0.08271	0.00899	1.03056	0.25785	0.00727	1.07665	0.26369	0.00722	1.07762
0.09105	0.00891	1.03368	0.09963	0.00882	1.03682	0.26976	0.00716	1.07852	0.27588	0.00710	1.07939
0.10856	0.00874	1.03996	0.11794	0.00864	1.04315	0.28213	0.00704	1.08024	0.28899	0.00697	1.08113
0.12786	0.00855	1.04635	0.13805	0.00845	1.04951	0.29556	0.00690	1.08193	0.30230	0.00684	1.08273
0.14942	0.00834	1.05298	0.16082	0.00822	1.05604	0.30918	0.00677	1.08350	0.31620	0.00670	1.08426
0.17259	0.00811	1.05923	0.18509	0.00799	1.06232	0.32336	0.00663	1.08499	0.33107	0.00656	1.08573
0.19880	0.00785	1.06552	0.21265	0.00772	1.06841	0.33857	0.00648	1.08641			
					$x_B^0 = 0.01870$						
0	0.01870	0.98496	0.00511	0.01860	0.98705	0.20836	0.01480	1.06286	0.21496	0.01468	1.06426
0.01048	0.01850	0.99007	0.01594	0.01840	0.99308	0.22124	0.01456	1.06551	0.22859	0.01443	1.06702
0.02149	0.01830	0.99606	0.02742	0.01819	0.99918	0.23562	0.01429	1.06833	0.24233	0.01417	1.06951
0.03342	0.01807	1.00227	0.03964	0.01796	1.00539	0.24920	0.01404	1.07069	0.25621	0.01391	1.07186
0.04621	0.01784	1.00859	0.05282	0.01771	1.01173	0.26336	0.01378	1.07299	0.27212	0.01361	1.07435
0.06059	0.01757	1.01535	0.06783	0.01743	1.01848	0.27965	0.01347	1.07542	0.28743	0.01333	1.07648
0.07521	0.01729	1.02165	0.08314	0.01715	1.02494	0.29536	0.01318	1.07750	0.30353	0.01302	1.07850
0.09119	0.01699	1.02816	0.09961	0.01684	1.03138	0.31197	0.01287	1.07948	0.32058	0.01271	1.08042
0.10849	0.01667	1.03466	0.11769	0.01650	1.03792	0.32942	0.01254	1.08132	0.33859	0.01237	1.08221
0.12729	0.01632	1.04116	0.13726	0.01613	1.04437	0.34791	0.01219	1.08306	0.35758	0.01201	1.08389
0.14769	0.01594	1.04757	0.15876	0.01573	1.05077						
0.17018	0.01552	1.05389	0.18234	0.01529	1.05701						
0.19497	0.01505	1.06003	0.20828	0.01481	1.06300						
					$x_B^0 = 0.02980$						
0	0.02980	0.98209	0.00550	0.02964	0.98524	0.21696	0.02333	1.05971	0.22225	0.02318	1.06080
0.01129	0.02946	0.98971	0.01720	0.02929	0.99313	0.22770	0.02301	1.06171	0.23318	0.02285	1.06267
0.02338	0.02910	0.99622	0.02984	0.02891	0.99933	0.23869	0.02269	1.06372	0.24445	0.02252	1.06478
0.03637	0.02872	1.00245	0.04333	0.02851	1.00560	0.25023	0.02234	1.06581	0.25624	0.02216	1.06684
0.05036	0.02830	1.00869	0.05777	0.02808	1.01183	0.26277	0.02197	1.06794	0.26898	0.02178	1.06885
0.06556	0.02785	1.01412	0.07353	0.02761	1.01821	0.27530	0.02160	1.06985	0.28180	0.02140	1.07081
0.08184	0.02736	1.02151	0.09124	0.02708	1.02548	0.28838	0.02121	1.07173	0.29513	0.02101	1.07267
0.10028	0.02681	1.02826	0.10972	0.02653	1.03154	0.30202	0.02080	1.07358	0.30906	0.02059	1.07446
0.11956	0.02624	1.03479	0.12988	0.02593	1.03808	0.31630	0.02037	1.07534	0.32365	0.02016	1.07619
0.14063	0.02561	1.04137	0.15193	0.02827	1.04465	0.33118	0.01993	1.07703	0.33889	0.01970	1.07784
0.16370	0.02492	1.04788	0.17616	0.02455	1.05112	0.34682	0.01946	1.07864	0.35487	0.01922	1.07940
0.18922	0.02416	1.05428	0.20365	0.02373	1.05769	0.36312	0.01898	1.08014	0.37160	0.01873	1.08087
0.21813	0.02330	1.06062	0.23338	0.02285	1.06358	0.38030	0.01847	1.08158			
					$x_B^0 = 0.03780$						
0	0.03780	0.98028	0.00575	0.03758	0.97990	0.20122	0.03019	1.05191	0.20703	0.02997	1.05342
0.01162	0.03736	0.98450	0.01761	0.03713	0.98776	0.21232	0.02977	1.05447	0.21786	0.02956	1.05566
0.02387	0.03690	0.99081	0.03041	0.03665	0.99428	0.22344	0.02935	1.05683	0.22904	0.02914	1.05796
0.03720	0.03639	0.99769	0.04408	0.03613	1.00106	0.23488	0.02892	1.05910	0.24084	0.02870	1.06023
0.05136	0.03586	1.00446	0.05886	0.03558	1.00770	0.24682	0.02847	1.06133	0.25299	0.02824	1.06243
0.06673	0.03528	1.01109	0.07479	0.03497	1.01430	0.25937	0.02800	1.06352	0.26573	0.02776	1.06450
0.08318	0.03466	1.01759	0.09204	0.03432	1.02091	0.27237	0.02750	1.06563	0.27907	0.02725	1.06665
0.10119	0.03398	1.02422	0.11073	0.03361	1.02754	0.28594	0.02699	1.06767	0.29293	0.02673	1.06867
0.12066	0.03324	1.03081	0.13108	0.03285	1.03411	0.30015	0.02645	1.06965	0.30748	0.02618	1.07062
0.14208	0.03243	1.03745	0.15347	0.03200	1.04071	0.31500	0.02589	1.07156	0.32269	0.02560	1.07250

TABLE 5 (Continued)

x_D	x_B	d/g cm^{-3}	x_D	x_B	d/g cm^{-1}	x_D	x_B	d/g cm^{-3}	x_D	x_B	d/g cm^{-1}
					$x_B^0 = 0.03780$						
0.16535	0.03155	1.04394	0.17791	0.03108	1.04718	0.33060	0.02530	1.07345	0.33865	0.02500	1.07434
0.19107	0.03058	1.05038	0.20500	0.03005	1.05355	0.34697	0.02468	1.07520	0.35537	0.02437	1.07604
0.21960	0.02950	1.05664	0.23498	0.02892	1.05965	0.36406	0.02404	1.07686			
					$x_B^0 = 0.05820$						
0	0.05820	0.96537	0.00592	0.05786	0.96800	0.10395	0.05215	1.01293	0.11356	0.05159	1.01638
0.01194	0.05750	0.97137	0.01808	0.05715	0.97468	0.12368	0.05100	1.01986	0.13400	0.05040	1.02325
0.02466	0.05676	0.97812	0.03134	0.05638	0.98154	0.14490	0.04977	1.02669	0.15632	0.04910	1.03012
0.03809	0.05598	0.98488	0.04526	0.05557	0.98832	0.16821	0.04841	1.03352	0.18065	0.04769	1.03693
0.05266	0.05513	0.99176	0.06110	0.05464	0.99596	0.19370	0.04693	1.04025	0.20737	0.04613	1.04356
0.06906	0.05418	0.99913	0.07736	0.05370	1.00261	0.22174	0.04529	1.04681	0.23677	0.04442	1.04998
0.08582	0.05321	1.00603	0.09475	0.05269	1.00949						
					$x_B^0 = 0.06925$						
0.00214	0.06910	0.96729	0.00852	0.06866	0.96792	0.13926	0.05961	1.02098	0.15131	0.05877	1.02527
0.01587	0.06815	0.97122	0.02269	0.06768	0.97515	0.16470	0.05784	1.02943	0.18272	0.05660	1.03464
0.03165	0.06706	0.97965	0.03866	0.06657	0.98023	0.020243	0.05523	1.03985	0.21965	0.05404	1.04395
0.04615	0.06605	0.98581	0.05372	0.06553	0.98952	0.23649	0.05287	1.04762	0.25078	0.05188	1.05017
0.06175	0.06497	0.99288	0.07001	0.06440	0.99618	0.26584	0.05084	1.05293	0.28274	0.04967	1.05598
0.07894	0.06381	0.99956	0.08735	0.06320	1.00293	0.30705	0.04799	1.06005	0.32436	0.04679	1.06232
0.09675	0.06255	1.00631	0.10631	0.06189	1.00964	0.34319	0.04548	1.06474	0.36265	0.04414	1.06691
0.11802	0.06108	1.01480	0.12845	0.06036	1.01754						
					$x_B^0 = 0.08000$						
0.00220	0.07982	0.95968	0.00872	0.07930	0.96170	0.14967	0.06803	1.02207	0.16098	0.06712	1.02547
0.01538	0.07877	0.96512	0.02448	0.07804	0.96974	0.17384	0.06609	1.02937	0.18628	0.06510	1.03244
0.03155	0.07748	0.97328	0.03892	0.07689	0.97740	0.19922	0.06406	1.03580	0.21715	0.06263	1.04034
0.04760	0.07619	0.98151	0.05945	0.07524	0.98599	0.23200	0.06144	1.04363	0.25179	0.05986	1.04782
0.06756	0.07460	0.99155	0.07686	0.07385	0.99655	0.26786	0.05857	1.05083	0.28973	0.05682	1.05476
0.08745	0.07300	0.99952	0.09635	0.07229	1.00358	0.30760	0.05539	1.05757	0.32529	0.05398	1.05999
0.10577	0.07154	1.00709	0.11552	0.07076	1.01068	0.34461	0.05243	1.06258	0.36496	0.05080	1.06500
0.12811	0.06975	1.01529	0.13870	0.06890	1.01857						
					$x_B^0 = 0.09000$						
0	0.09000	0.94660	0.00676	0.08939	0.94959	0.11927	0.07927	1.00075	0.13026	0.07828	1.00460
0.01343	0.08879	0.95312	0.02067	0.08814	0.95704	0.14162	0.07725	1.00844	0.15351	0.07618	1.01229
0.02801	0.08748	0.96087	0.03545	0.08681	0.96467	0.16601	0.07506	1.01613	0.18054	0.07375	1.02065
0.04341	0.08609	0.96867	0.05143	0.08537	0.97252	0.19630	0.07233	1.02509	0.21823	0.07036	1.03152
0.05993	0.08461	0.97645	0.06964	0.08373	0.98127	0.23374	0.06896	1.03535	0.24887	0.06760	1.03861
0.07954	0.08242	0.98778	0.08885	0.08200	0.98971	0.26521	0.06613	1.04204	0.28178	0.06464	1.04515
0.09853	0.08113	0.99309	0.10873	0.08021	0.99695						

changes in chemical potentials, μ_i (i = B, D, or W). Thus

$$x_B\Delta\mu_B + x_D\Delta\mu_D + x_W\Delta\mu_W = 0 \qquad \text{(A1)}$$

where Δ represents the small but finite change associated with the change from the "up" element down by one element. The chemical potentials in eq A1 can be rewritten in terms of the partial pressures as

$$x_B\{\ln(p_B/p_B^U)\} + \{(x_D + x_D^U)/2\}\{\ln(p_D/p_D^U)\} + \{(x_W + x_W^U)/2\}\{\ln(p_W/p_W^U)\} = 0 \qquad \text{(A2)}$$

Similarly for the change from the "left" element

$$\{(x_B + x_B^L)/2\}\{\ln(p_B/p_B^L)\} + x_D\{\ln(p_D/p_D^L)\} + \{(x_W + x_W^L)/2\}\{\ln(p_W/p_W^L)\} = 0 \qquad \text{(A3)}$$

$$p = p_B + p_D + p_W \qquad \text{(A4)}$$

Since p_i^U and p_i^L are known (where i = B, D, or W), eqs A2 − A4 provide a route to calculate the three unknowns, p_B, p_D, and p_W. Eliminating p_D and p_W from eq A2−A4 yields

$$p_B + \exp(Y)\,(p_B)^X + \exp(V)\,(p_B)^Z = p \qquad \text{(A5)}$$

where X, Y, Z, and V are calculated with known x_i's and p_i's (see Appendix II). Equation A5 is then solved for p_B numerically. p_D and p_W are in turn calculated. The solutions for this element will provide the basis for solving the subsequent elements. This calculation procedure is applicable only for the elements with $m \geq 3$ and $n \geq 3$. For the elements in the second column, $n = 2$, or the second row, $m = 2$, the values of p_B^L or p_D^U are inevitably zero and hence eqs A2 and A3 become undeterministic. Therefore the elements (m, 2), and (2, n) must be estimated independently to initiate the above calculation procedure. A similar situation occurs in solving a binary system by the Boissonnas method.

The first column of Table 2, $x_B = 0$, contains the p data for the binary DMSO−H_2O mixtures, for which the partial pressures were solved by the Boissonnas method,[6] a numerical iteration method based on the Duhem−Margules relation for a binary system. Similarly the first row of Table 2, $x_D = 0$, contains the results of the binary TBA−H_2O.[4,5,15] To start iteration based on the Boissonnas method, the partial pressures of the very first and the most dilute solution must be guessed independently. It is customary to assume that the most dilute point is in the Henry's law region and hence the major component, H_2O in this case, obeys Raoult's law, which may be in fact in error. However, the strength of the Boissonnas method for a binary system is its self-correcting nature,[15] by which the error caused by the wrong guess is self-corrected for as the successive data point is calculated, and the results seem to eventually reach correct values. In the binary TBA−H_2O, for the step of successive data points of $\Delta x_B \approx 0.002$, the third point converged

onto the smooth extension of p_B,[4,5] while for $\Delta x_B \approx 0.00008$, convergence was observed at the seventh point.[15]

Equivalently, for the ternary TBA−DMSO−H_2O system, partial pressures must be estimated independently in the second column (m, 2) ($x_B = 0.005$) and in the second row (2, n) ($x_D = 0.01$), where the mole fraction of either TBA or DMSO takes its lowest nonzero value. We proceeded in the following manner. Noting that p_D is 2 orders of magnitude smaller than p_B and p_W, we assumed that p_D stays constant for the change from the first column ($x_B = 0$) to the second ($x_B = 0.05$) with a fixed value of x_D. Furthermore, we assumed that the ratio of $p_W{}^L/p_W$ remains the same as that of the first row (for a binary TBA−H_2O) throughout of the entire second column. Namely, we assumed that nonideal TBA−DMSO interactions are negligible under these dilute conditions, and hence TBA−H_2O interactions, even in the presence of DMSO, remain the same as that of the binary mixtures. As will become apparent, these assumptions are not unreasonable. p_B is then calculated by eq A4. The results are shown in the second column, $x_B = 0.005$, of Table 3.

The partial pressures in the second row must also be estimated in some way. It turned out that a wrong guess on p_D for the second row (the most dilute x_D) of the third and the subsequent columns causes oscillation in the values of p_B and p_W as the iteration based on eqs A2−A5 proceeds downward in the given column. In a binary system, an error in one component may be corrected for by the second component in the Gibbs−Duhem relation, as was evident for TBA− and DMSO−H_2O binary systems.[4−6,15] In a ternary mixture, on the other hand, there are two terms to correct for an error in one component. This additional degree of freedom seems to cause an over correction and oscillation in p_B and p_W toward the bottom of the column. This property for a ternary mixture can be taken advantage of in monitoring a correct guess in p_D of the second row of each column. The absolute uncertainty in p is estimated to be ±0.01 Torr. Hence the same uncertainty is expected for the partial pressures, p_D, p_B, and p_W. However, for the reasons mentioned below, the value of p_D in the second row must be estimated more precisely than ±0.01 Torr. As is evident from eqs A2 and A3, the present method uses the logarithm of each partial pressures. Therefore, the initial guess in p_D for the second row must have the same as or preferably more significant figures than p_B and p_W. Indeed, when p_B is small with 3 significant figures at small x_B, p_D in the second row (the most dilute solution in x_D) must be guessed with 4 significant figures before the entire column with fixed x_B is successfully iterated without oscillation. At higher values of x_B where p_B's are large with 4 significant figures, p_D must be guessed with 5−6 significant figures. Thus, it is clear that all through this process the uncertainty does not increase.

In summary, we solved the third and subsequent columns as follows. We guessed the value of p_D for the second row ($x_D = 0.01$) and the third column ($x_B = 0.01$) to a similar value as the one to the left element ($x_B = 0.005$, $x_D = 0.01$). Then p_B and p_W in the second row are calculated as a semibinary mixture using eqs A3 and A4. The subsequent rows of this column are now solved by eqs A2−A5. If the original guess of p_D in the second row is grossly wrong, the resulting values of p_B oscillate toward the bottom of the column and become negative in worst cases. A revised guess is then given to p_D in the second row, and the procedure is repeated until the correct guess to the right significant figures is reached. A number of iterations were required in an orderly fashion to obtain p_D in the right number of significant figures.

The values of partial pressures thus obtained are listed in Table 3. We note that the estimated partial pressures in the second column could very well be in error, but that such errors would be self-corrected for in the subsequent columns as the iteration proceeded. The elements in the second row, though estimated by the criterion mentioned above, were subsequently calculated as a semibinary mixture. Hence, possible error in element (2, 2) may not be properly self-corrected for in the subsequent elements (2, n) in the second row. In element (3, 3), which was calculated using the data in elements (3, 2) and (2, 3), the resulting partial pressures could be still affected by possible errors in the elements (3, 2) and (2, 3). Thus, the data of the entire second column ($x_B = 0.005$), the entire second row ($x_D = 0.01$), and the element (3, 3) or ($x_B = 0.01$, $x_D = 0.03$), appearing in italics in Table 3, will not be used in the subsequent analysis.

Table 4 shows the values of $\mu_{DB}{}^E$ and $\mu_{BD}{}^E$ calculated using the data in Table 3 for $x_B > 0.05$ and $x_D > 0.01$ as

$$\mu_{DB}{}^E = N(\partial\mu_D{}^E/\partial n_B) = (1 - x_B{}^M)(\delta\mu_D{}^E/\delta x_B) - x_D{}^M(\delta\mu_D{}^E/\delta x_D)$$

with $\mu_D{}^E = RT\ \ln(p_D/x_D p_D{}^o)$, where $x_B{}^M$ is the value of x_B between the neighbor columns, and $(\delta\mu_D{}^E/\delta x_B)$ signifies the differential taken using the values of neighbor columns. $x_D{}^M$ and $(\delta\mu_D{}^E/\delta x_D)$ are evaluated using the pertinent data of neighboring rows. $\mu_{BD}{}^E$ is also calculated in the same way

$$\mu_{BD}{}^E = N(\partial\mu_B{}^E/\partial n_D) = (1 - x_D{}^M)(\delta\mu_B{}^E/\delta x_D) - x_B{}^M(\delta\mu_B{}^E/\delta x_B)$$

Table 4 indicates that these two sets are numerically consistent within ± 0.03 kJ mol $^{-1}$. This is remarkable considering that $\mu_D{}^E$ is calculated from p_D, the value of which varies from 0.0017 to 0.08 Torr, while the value of p_B varies from 7 to 15 Torr, which was used to calculate $\mu_B{}^E$. Despite this large difference in the partial pressures and hence in the resulting excess chemical potentials for DMSO and TBA, the cross derivatives, $\mu_{DB}{}^E$ and $\mu_{BD}{}^E$, calculated from them are consistent within ± 0.03 kJ mol $^{-1}$! This gives a confidence in the values of chemical potential and in the present numerical method employed in evaluating partial pressures. Furthermore, the uncertainty in $\mu_B{}^E$ and $\mu_D{}^E$ is at worst ±0.03 kJ mol $^{-1}$ and is more likely better by at least 10-fold.

Appendix II

Calculating p_D and p_W from eqs A2 and A3

$$\ln p_W = X \ln p_B + Y \tag{A6}$$

$$\ln p_D = Z \ln p_B + V \tag{A7}$$

where

$$X = (x_D{}^m x_B{}^m - x_D x_B)/Q$$

$$Y = (x_D T^U - x_D{}^m T^L)/Q$$

$$Z = \{x_B(1 - x_B{}^m - x_D) - x_B{}^m(1 - x_B - x_D{}^m)\}/Q$$

$$V = \{(1 - x_B - x_D{}^m)T^L - (1 - x_B{}^m - x_D)T^U\}/Q$$

with

$$x_B^m = (x_B + x_B^L)/2$$

$$x_D^m = (x_D + x_D^U)/2$$

$$T^L = x_B^m \ln p_B^L + x_D \ln p_D^L + (1 - x_B^m - x_D) \ln p_W^L$$

$$T^U = x_B \ln p_B^U + x_D^m \ln p_D^U + (1 - x_B - x_D^m) \ln p_W^U$$

$$Q = x_D (1 - x_B - x_D^m) - x_D^m (1 - x_B^m - x_D)$$

Insertion of eqs A6 and A7 into eq A4 yields eq A5.

References and Notes

(1) Koga, Y. *Can. J. Chem.* **1986**, *64*, 206.
(2) Koga, Y. *Can. J. Chem.* **1988**, *66*, 1187.
(3) Koga, Y. *Can. J. Chem.* **1988**, *66*, 3171.
(4) Koga, Y.; Siu, W. W. Y.; Wong, T. Y. H. *J. Phys. Chem.* **1990**, *94*, 7700.
(5) Koga, Y.; Wong, T. Y. H.; Siu, W. W. Y. *Thermochim. Acta* **1990**, *169*, 27.
(6) Lai, J. T. W.; Lau, F. W.; Robb, D.; Westh, P.; Nielsen, G.; Trandum, Ch.; Hvidt, Aa.; Koga, Y. *J. Solution Chem.* **1995**, *24*, 89.
(7) Koga, Y. *J. Crystallogr. Soc. Jpn.* **1995,** *37*, 172.
(8) Koga, Y. *J. Phys. Chem.* **1996**, *100*, 5172.
(9) Stanley, H. E.; Teixeira, J. *J. Chem. Phys.* **1980,** *73*, 3404.
(10) Blumberg, R. L.; Stanley, H. E.; Geiger, A.; Mausbach, P. *J. Chem. Phys.* **1984,** *80*, 5230.
(11) Lumry, R.; Rajender, S. *Biopolymers* **1970,** *9*, 1125.
(12) Sakurai, M. *Bull. Chem. Soc. Jpn.* **1987**, *60*, 1.
(13) Koga, Y.; Kristiansen, J.; Hvidt, Aa. *J. Chem. Thermodyn.* **1993,** *25*, 51.
(14) Koga, Y. *J. Phys. Chem.* **1992,** *96*, 10466.
(15) Koga, Y. *J. Phys. Chem.* **1995,** *99*, 6231 and 12370.
(16) Koga, Y.; Westh, P.; Trandum, Ch.; Haynes, C. A. *Fluid Phase Equilib.* **1997,** *136*, 207.
(17) Lovelock, J. E.; Bishop, M. W. H. *Nature* **1959,** *183*, 1394.
(18) Timasheff, S. N. *Biochemistry* **1992,** *31*, 9857.
(19) Withers, L. A. *The Effects of Low Temperature on Biological Systems*; Grout, B. B. W., Morris, G. J., Eds.; Edwards Arnold Publishers: London, 1987.
(20) Arakawa, T.; Carpenter, J. F.; Kita, Y. A.; Crowe, J. H. *Cryobiology* **1990,** *27*, 401.
(21) Fahy, G. M.; Lilley, T. H.; Linsdell, H.; Douglas, M. S. J.; Meryman, H. T. *Cryobiolology* 1990, *27*, 247.
(22) Fujita, Y.; Izumiguchi, S.; Noda, Y. *Int. J. Peptide Protein Res.* **1982,** *19*, 25.
(23) Lehman, M. S.; Stanfield, R. F. D. *Biochemistry* **1989,** *28*, 7028.
(24) Westh, P. *J. Phys. Chem.* **1994**, *98*, 3222.
(25) Westh, P.; Koga, Y. *J. Phys. Chem.* **1996,** *100*, 433.
(26) Mastroianni, M. J.; Pikal, M. J.; Lindenbaum, S. *J. Phys. Chem.* **1972,** *76*, 3050.
(27) Koga, Y.; Westh, P.; Sawamura, S.; Taniguchi, Y. *J. Chem. Phys.* **1996,** *105*, 2028.
(28) Nishikawa, K.; Yoshino, K.; Koga, Y. To be published.
(29) Abbott, M. M.; Floess, J. K.; Walsh Jr., G. E.; Van Ness, H. C. *AIChE J.* **1975,** *21*, 72.
(30) Yaacobi, M.; Ben-Naim, A. *J. Solution Chem.* **1973**, *2*, 425.
(31) Ben-Naim, A.; Yaacobi, M. *J. Phys. Chem.* **1975,** *79*, 1263.
(32) Oakenfull, D. G.; Fenwick, D. E. *J. Phys. Chem.* **1974,** *78*, 1759.
(33) Oakenfull, D.; Fenwick, D. E. *Aust. J. Chem.* **1977,** *30*, 741.
(34) Oakenfull, D.; Fenwick, D. E. *J. Chem. Soc., Faraday Trans. 1* **1979,** *75*, 636.
(35) Tanaka, S. H.; Yoshihara, H I.; Ho, A. W.-C.; Lau, F. W.; Westh, P.; Koga, Y. *Can. J. Chem.* **1996,** *74*, 713.
(36) Ben-Naim, A. *J. Chem. Phys.* **1971,** *54*, 1387, 3696; **1972**, *57*, 5257.